Phase Noise in Oscillators: A Unifying Theory and Numerical Methods for Characterization

Alper Demir, Amit Mehrotra, and Jaijeet Roychowdhury

***Abstract*—Phase noise is a topic of theoretical and practical interest in electronic circuits, as well as in other fields, such as optics. Although progress has been made in understanding the phenomenon, there still remain significant gaps, both in its fundamental theory and in numerical techniques for its characterization. In this paper, we develop a solid foundation for phase noise that is valid for any oscillator, regardless of operating mechanism. We establish novel results about the dynamics of stable nonlinear oscillators in the presence of perturbations, both deterministic and random. We obtain an exact nonlinear equation for phase error, which we solve without approximations for random perturbations. This leads us to a precise characterization of timing jitter and spectral dispersion, for computing which we develop efficient numerical methods. We demonstrate our techniques on a variety of practical electrical oscillators and obtain good matches with measurements, even at frequencies close to the carrier, where previous techniques break down. Our methods are more than three orders of magnitude faster than the brute-force Monte Carlo approach, which is the only previously available technique that can predict phase noise correctly.**

***Index Terms*—Circuit simulation, Fokker-Planck equations, nonlinear oscillators, oscillator noise, phase noise, stochastic differential equatioons, timing jitter.**

I. Introduction

OSCILLATORS are ubiquitous in physical systems, especially electronic and optical ones. For example, in radio frequency (RF) communication systems they are used for frequency translation of information signals and for channel selection. Oscillators are also present in digital electronic systems which require a time reference, i.e., a clock signal, in order to synchronize operations.

Noise is of major concern in oscillators, because introducing even small noise into an oscillator leads to dramatic changes in its frequency spectrum and timing properties. This phenomenon, peculiar to oscillators, is known as phase noise or timing jitter. A perfect oscillator would have localized tones at discrete frequencies (i.e., harmonics), but any corrupting noise spreads these perfect tones, resulting in high power levels at neighboring frequencies. This effect is the major contributor to undesired phenomena such as interchannel interference, leading to increased bit error rates (BER's) in RF communication systems. Another manifestation of the same phenomenon, jitter, is important in clocked and sampled-data systems. Uncertainties in switching instants caused by noise lead to synchronization problems. Characterizing how noise affects oscillators is therefore crucial for practical applications. The problem is challenging, since oscillators constitute a special class among noisy physical systems. Their autonomous nature makes them unique in their response to perturbations.

Considerable effort has been expended over the years in understanding phase noise and in developing analytical, computational and experimental techniques for its characterization (see Section III for a brief review). Despite the importance of the problem and the large number of publications on the subject, a consistent and general treatment and computational techniques based on a sound theory appear to be still lacking. In this work, we provide a novel, rigorous theory for phase noise and derive efficient numerical methods for its characterization. Our techniques and results are general. They are applicable to any oscillatory system, electrical (resonant, ring, relaxation, etc.) or otherwise (gravitational, optical, mechanical, biological, etc.). The main ideas behind our approach and our contributions are outlined in Section II. We apply our numerical techniques to a variety of practical oscillator designs and obtain good matches against measurements. Our computations are efficient. Speedups of a factor of 1800 were obtained against the Monte Carlo method, which is the only previously available technique needed to produce similar results.

The paper is organized as follows. In Section II we present an overview of the main results of the paper and in Section III we give a brief review of the previous work. In Section IV we introduce some basic mathematical notions about oscillators. In Section V we consider the traditional approach (linearization) to analyzing perturbed nonlinear systems and show how this procedure is not consistent for autonomous oscillators. In Section VI we derive a nonlinear equation that exactly captures how perturbations result in phase noise. In Section VII we solve this equation with random perturbations and arrive at a stochastic description of phase deviation, from which we derive timing jitter. Next, in Section VIII, we use this stochastic characterization to calculate the correct shape of the oscillator's spectrum with phase noise. In Section IX we derive several quantities commonly used in oscillator design to quantify jitter and spectral properties. In Section X we address the problem of computing these quantities efficiently, even for large circuits. We develop both time- and frequency-domain numerical methods that can easily be implemented in existing simulators. Finally, in Section XI, we apply our methods to a variety of practical electrical oscillators and we also indicate how our methods can be directly incorporated into existing

Manuscript received April 29, 1998; revised August 17, 1999. This paper was recommended by Associate Editor P. Rentrop.

A. Demit and J. Roychowdhury are with the Design Principles Research Department, Bell Laboratories, Lucent Technologies, Murray Hill, NJ 07974 USA.

A. Mehrotra is with the Department of Electrical and Computer Engineering, University of Illinois, Urbana-Champaign, IL 61801 USA.

Publisher Item Identifier S 1057-7122(00)03972-6.

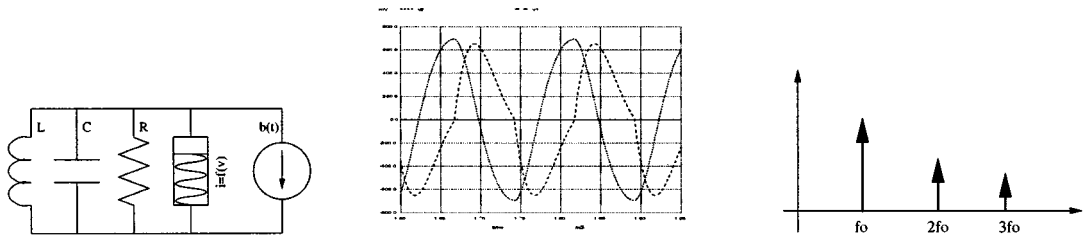

Fig. 1. Oscillator and waveforms.

design methodologies. Appendices A–C describe several mathematical concepts, definitions, and results used throughout the paper.

II. Overview and Main Contributions

In this section, we first outline the flow of the rest of the paper and describe the basic concepts behind our treatment of phase noise. We then discuss how our approach has a natural state-space or phase-plane interpretation. We summarize the novel aspects of our work at the end.

A. Outline of Main Results

Consider the oscillator shown in Fig. 1(a), consisting of a lossy LC circuit with an amplitude-dependent gain provided by the nonlinear resistor. The nonlinear resistor has a negative resistance region which pumps energy into the circuit when the capacitor voltage drops, thus maintaining stable oscillation. A current source $b(t)$ is also present, representing external perturbations due to noise. When there is no perturbation, i.e., $b(t)$ is zero, the oscillator oscillates with a perfectly periodic signal $x_s(t)$ (a vector consisting of the capacitor voltage and the inductor current), shown in Fig. 1(b). In the frequency domain, the unperturbed waveform consists of a series of impulses at the fundamental and harmonics of the time period, as shown in Fig. 1(c).

Although our eventual intent is to understand the response of the oscillator when $b(t)$ is random noise, it is useful to consider first the case when $b(t)$ is a known deterministic signal. We carry out a rigorous analysis of this case in Section VI and obtain the following results.

1) The unperturbed oscillator's periodic response $x_s(t)$ is modified to $x_s(t+\alpha(t))+y(t)$ by the perturbation where the following holds.
   a) $\alpha(t)$ is a changing time shift or phase deviation in the periodic output of the unperturbed oscillator.
   b) $y(t)$ is an additive component, which we term the orbital deviation, to the phase-shifted oscillator waveform.
2) $\alpha(t)$ and $y(t)$ can always be chosen such that the following holds.
   a) $\alpha(t)$ will, in general, keep increasing with time even if the perturbation $b(t)$ is always small.
   b) The orbital deviation $y(t)$, on the other hand, will always remain small.

These results concretize existing intuition amongst designers about oscillator operation. Our proof of these facts is mathematically rigorous. Furthermore, we derive equations for $\alpha(t)$ and $y(t)$ which lead to qualitatively different results about phase noise compared to previous attempts. This is because our results are based on a new nonlinear perturbation analysis that is valid for oscillators, in contrast to previous approaches that rely on linearization. We show in Section V that analysis based on linearization is not consistent for oscillators and results in nonphysical predictions.

Next, we consider the case where the perturbation $b(t)$ is random noise. This situation is important for determining practical figures of merit such as zero-crossing jitter and spectral purity (i.e., spreading of the power spectrum).[1] Jitter and spectral spreading are, in fact, closely related and both are determined by the manner in which $\alpha(t)$, now also a random process, spreads with time. We consider random perturbations in detail in Sections VII and VIII and establish the following.

1) The average spread of the jitter (mean-square jitter) increases precisely linearly with time.
2) The power spectrum of the perturbed oscillator is a Lorentzian[2] about each harmonic.
3) A single scalar constant c is sufficient to describe jitter and spectral spreading in a noisy oscillator.
4) The oscillator's output is a stationary stochastic process.

These results have important implications. The Lorentzian shape of the spectrum implies that the power spectral density (PSD) at the carrier frequency and its harmonics has a finite value and that the total carrier power is preserved despite spectral spreading due to noise. Previous analyses based on linear time-invariant (LTI) or linear time-varying (LTV) concepts erroneously predict infinite noise power density at the carrier, as well as infinite total integrated power. That the oscillator output is stationary is surprising at first sight since oscillators are nonlinear systems with periodic swings, hence, it might be expected that output noise power would change periodically as in forced systems. However, it must be remembered that while forced systems are supplied with an external time reference (through the forcing), oscillators are not. Cyclostationarity in the oscillator's output would, by definition, imply a time reference. Hence, the stationarity result reflects the fundamental fact that noisy autonomous systems cannot provide a perfect time reference.

Next, in Section X, we apply the theory above to develop correct computational techniques that are efficient for practical circuits. We present two new numerical methods (in the time

[1]The deterministic perturbation case is also of interest, for, e.g., phenomena such as mode locking in forced oscillators. We consider this case elsewhere [1].

[2]A Lorentzian is the shape of the squared magnitude of a one-pole lowpass filter transfer function.

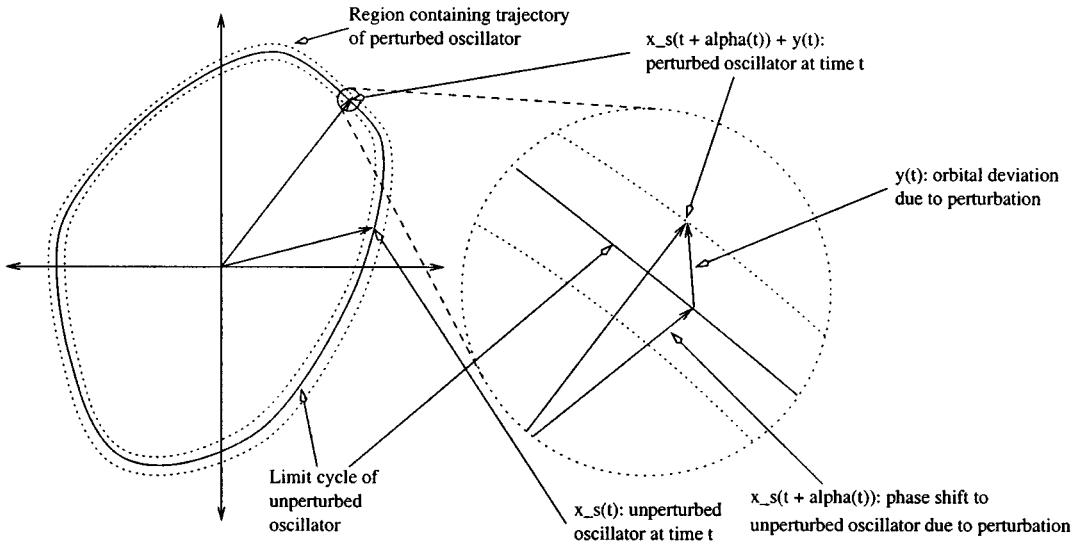

Fig. 2. Oscillator trajectories.

and frequency domains) for jitter/spectral dispersion, with the following features.

1) The methods require only a knowledge of the steady state of the unperturbed oscillator and the values of the noise generators.
2) Large circuits are handled efficiently, i.e., computation/memory scale linearly with circuit size.
3) The separate contributions of noise sources and the sensitivity of phase noise to individual circuit devices and nodes can be obtained easily.

Finally, in Section XI, we use our theory and numerical methods to analyze several oscillators and compare the results against measurements. We obtain good matches, even at frequencies close to the carrier, unlike most previous analyses. Our numerical methods are more than three orders of magnitude faster than Monte Carlo simulations, the only alternative method for producing qualitatively correct predictions. The brute-force Monte Carlo technique is the only previously available analysis method, apart from ours, that is not based on linearization.

B. State-Space Interpretations of Phase and Orbital Deviation

The phase and orbital deviations have intuitive interpretations when the oscillator's response is viewed in the state-space or phase plane. In Fig. 2, the voltage $v(t)$ across the capacitor is plotted against the current $i(t)$ through the inductor. The trace for the unperturbed oscillator forms a closed curve since this waveform is perfectly periodic. When the oscillator is perturbed, this periodicity is lost. For stable oscillators, however, the perturbed trajectory remains within a small band around the unperturbed trajectory, as shown.

The closeness of the perturbed and unperturbed trajectories in the phase plane does not imply that the time-domain waveforms are also close to each other. The points on the perturbed and unperturbed trajectory corresponding to a given time t will, in general, be far from each other, as illustrated in Fig. 2. However, the waveform of the perturbed oscillator does remain close to the unperturbed waveform after it is time shifted by $\alpha(t)$. In the figure, this time or phase shift results in the difference between the unperturbed point $x_s(t)$ and the phase component $x_s(t + \alpha(t))$ of the perturbed trajectory. The orbital deviation $y(t)$ due to the perturbation is also shown.

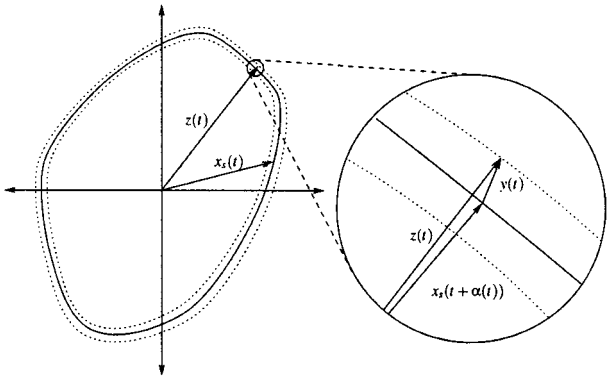

Fig. 3. Limit cycle and excursion due to perturbation.

It is shown in Section VI that $\alpha(t)$ grows very much like the integral of the perturbation. For a constant perturbation, for example, $\alpha(t)$ is approximately a linear ramp. This indicates how the frequency of the oscillator can change due to perturbations, for a linearly increasing phase error is equivalent to a frequency error. It also suggests why cycle-to-cycle (i.e., per cycle) timing jitter is a constant quantity.

C. Main Contributions

Our treatment contains a number of advances over the previous state of the art. The main ones are the following.

- We present a rigorous nonlinear analysis of the perturbed oscillator. In contrast, previous analyses rely purely on linearizations. Our approach leads to a nonlinear differential equation for the phase shift $\alpha(t)$ that is qualitatively different from those based on linear analyses. We show, in fact, that linear analyses are not consistent (Section V).
- Our analysis and results apply to any oscillatory system described by differential equations, while

previous analyses are usually for special cases or classes of oscillators.

- We analyze the case of random perturbations rigorously and show that the following holds.

  The average spread of the phase error grows exactly linearly with time.

  The oscillator output with phase noise is stationary.

  A single scalar constant c suffices to characterize the timing jitter and spectral broadening due to phase noise.
- We develop efficient computational methods in the time and frequency domains for predicting phase noise. Our techniques are practical for large circuits. We obtain good matches between spectra predicted using our technique and measured results, even at frequencies close to the carrier and its harmonics, where most previous techniques break down. Our numerical techniques are much faster (three orders of magnitude) and also more accurate than the Monte Carlo methods.

III. Previous Work

A great deal of literature is available on the phase noise problem. Here we mention only some selected works from the fields of electronics and optics. Most investigations of electronic oscillators aim to provide insight into frequency-domain properties of phase noise in order to develop rules for designing practical oscillators; well-known references include [2]–[6]. Usually, these approaches apply LTI analysis to high-Q or quartz-crystal type oscillators designed using standard feedback topologies. Arguments based on deterministic perturbations are used to show that the spectrum of the oscillator response varies as $1/f^2$ times the spectrum of the perturbation. While often of great practical importance, such analyses often require large simplifications of the problem and skirt fundamental issues, such as why noisy oscillators exhibit spectral dispersion whereas forced systems do not.

Attempts to improve on LTI analysis have borrowed from LTV analysis methods for forced (nonoscillatory) systems (e.g., [7]–[10]). LTV analyses can predict spectra more accurately than LTI ones in some frequency ranges, however, LTV techniques for forced systems retain nonphysical artifacts of LTI analysis (such as infinite output power) and provide no real insight into the basic mechanism generating phase noise.

Oscillators that rely on abruptly switching elements, e.g., ring and relaxation oscillators, are more amenable to noise analysis. Perturbations cause variations in element delays or alter the time taken to reach switching thresholds, thus directly determining timing jitter. References [11]–[13] predict phase noise by using analytical techniques on idealized models of specific oscillator circuits. The mechanism of such oscillators suggests the fundamental intuition that timing or phase errors increase with time. However, this intuition does not extend naturally to other types of oscillators.

More sophisticated analysis techniques predominate in the domain of optics. Here, stochastic analysis is common and it is well known that phase noise due to white noise perturbations is described by a Wiener, or random walk, process. Although justifications of this fact are often based on approximations, precise descriptions of phase noise have been obtained for certain systems. In the seminal work of Lax [14], for example, an equation describing the growth of phase fluctuations with time is obtained for pumped lasers. The fact that a Wiener phase noise process leads to Lorentzian power spectra is also well established, e.g., [15] and [16]. However, a general theory is apparently not available even in this field.

Possibly the most general and rigorous treatment of phase noise to date has been that of Kärtner [17]. In this work, the oscillator response is decomposed into phase and magnitude components and a differential equation is obtained for phase error. By solving a linear small-time approximation to this equation with stochastic inputs, Kärtner obtains the correct Lorentzian spectrum for the PSD due to phase noise. Despite these advances certain gaps remain, particularly with respect to the derivation and solution of the differential equation for phase error.

Recently, Hajimiri [18], [19] has proposed a phase noise analysis based on a conjecture for decomposing perturbations into two (orthogonal) components, generating purely phase and amplitude deviations, respectively. While this intuition is similar to Kärtner's approach [17], other aspects of Hajimiri's treatment (e.g., stochastic characterization for phase deviation and the spectrum calculation) are essentially equivalent to LTV analysis. Unfortunately, the conjecture for orthogonally decomposing the perturbation into components that generate phase and amplitude deviations, while intuitively appealing, can be shown to be invalid [20]. Design intuition resulting from the conjecture about noise source contributions can also be misleading.

In summary, the available literature often identifies basic and useful facets of phase noise separately, but lacks a rigorous unifying theory clarifying its fundamental mechanism. Furthermore, existing numerical methods for phase noise are based on forced-system concepts which are inappropriate for oscillators and can generate incorrect predictions.

IV. Preliminaries

The dynamics of any autonomous system without undesired perturbations can be described by a system of differential equations. For notational simplicity, we use the state equation formulation throughout the paper to describe the dynamics of an autonomous system. The results and the numerical methods we present can be extended for the modified nodal analysis (MNA) formulation (differential-algebraic equations with index one) given by $d/dt\ q(x) + f(x) = 0$. Please see [21] and [22] for details. We have

$$\dot{x} = f(x) \tag{1}$$

where $x \in \mathbb{R}^n$ and $f(\cdot)$: $\mathbb{R}^n \rightarrow \mathbb{R}^n$. We assume that $f(\cdot)$ satisfies the conditions of the Picard–Lindelőf existence and uniqueness theorem for initial value problems [23]. We consider systems that have an asymptotically orbitally stable[3] (see Appendix A) periodic solution $x_s(t)$ (with period T) to (1), i.e., a stable

[3]After any small disturbance that does not persist, the system asymptotically settles back to the original limit cycle. See the Appendix A for a precise definition of this stability notion.

limit cycle in the n-dimensional solution space. We are interested in the response of such systems to a small state-dependent perturbation of the form $B(x)b(t)$ where $B(\cdot)$: $\mathbb{R}^n \rightarrow \mathbb{R}^{n\times p}$ and $b(\cdot)$: $\mathbb{R}\rightarrow\mathbb{R}^p$. Hence, the perturbed system is described by

$$\dot{x} = f(x) + B(x)b(t). \tag{2}$$

Let the exact solution of the perturbed system in (2) be $z(t)$.

V. Perturbation Analysis Using Linearization

The traditional approach to analyzing perturbed nonlinear systems is to linearize about the unperturbed solution, under the assumption that the resultant deviation[4] will be small. Let this deviation be $w(t)$, i.e., $z(t) = x_s(t) + w(t)$. Substituting this expression for $z(t)$ in (2), replacing $f(x_s(t) + w(t))$ by its first-order Taylor series expansion, approximating $B(x)$ with $B(x_s)$, [i.e., we use only the zeroth-order Taylor series term $B(x_s)\ b(t)$ which captures the modulation of the noise sources with the large signal steady state. Note that we ignore the first-order term in the expansion of $B(x)\ b(t)$ around $x_s(t)$, i.e., $dB(x_s)/dx\ w(t)\ b(t)$. This term is a high-order effect that captures the modulation of the noise sources by themselves and can be neglected for all practical purposes] and assuming that $w(t)$ is small, we obtain

$$\begin{aligned}\dot{w} &\approx \left.\frac{\partial f(x)}{\partial x}\right|_{x_s(t)} w(t) + B(x_s(t))b(t)\\ &= A(t)w(t) + B(x_s(t))b(t)\end{aligned} \tag{3}$$

where the Jacobian $A(t) = (\partial f(x)/\partial x)|_{x_s(t)}$ is T-periodic. Here, we used the fact that $x_s(t)$ satisfies (1). Now, we would like to solve for $w(t)$ in (3) to see if our assumption that it is small is indeed justified. For this, we use results from Floquet theory [23], [24] as follows (see Appendix B).[5]

The state transition matrix for the homogeneous part of (3) is given by (see Theorem B.1)

$$\Phi(t,\, s) = U(t)\exp(D(t-s))V(s) \tag{4}$$

where $U(t)$ is a T-periodic nonsingular matrix, $V(t) = U^{-1}(t)$ and $D = \text{diag}[\mu_1, \cdots, \mu_n]$, where μ_i are the Floquet (characteristic) exponents. $\exp(\mu_i T)$ are called the characteristic multipliers.

Remark 5.1: Let $u_i(t)$ be the columns of $U(t)$ and $v_i^T(t)$ be the rows of $V(t) = U^{-1}(t)$. Then $\{u_1(t), u_2(t), \cdots, u_n(t)\}$ and $\{v_1(t), v_2(t), \cdots, v_n(t)\}$ both span $\mathbb{R}^n$ and satisfy the biorthogonality conditions $v_i^T(t)\ u_j(t) = \delta_{ij}$ for every t. Note that, in general, $U(t)$ itself is not an orthogonal matrix.

Let us first consider the homogeneous part of (3), the solution of which is given by

$$\begin{aligned}w_H(t) &= U(t)\exp(Dt)V(0)w(0)\\ &= \sum_{i=1}^{n} u_i(t)\exp(\mu_i t)v_i^T(0)w(0)\end{aligned} \tag{5}$$

where $w(0)$ is the initial condition. Next, we will show that one of the terms in the summation in (5) does not decay with t.

Lemma 5.1:

- The unperturbed oscillator (1) has a nontrivial T-periodic solution $x_s(t)$ if and only if 1.0 is a characteristic multiplier of the homogeneous part of (3) or, equivalently, one of the Floquet exponents satisfies $\exp(\mu_i T) = 1.0$.
- The time-derivative of the periodic solution $x_s(t)$ of (1), i.e., $\dot{x}_s(t)$, is a solution of the homogeneous part of (3).

Proof: Since $x_s(t)$ is a nontrivial periodic solution of (1), it satisfies $\dot{x}_s(t) = f(x_s(t))$. Taking the time derivative of both sides of this equation, it follows immediately that $\dot{x}_s(t)$ satisfies $\dot{w} = A(t)w$, the homogeneous part of (3). Thus

$$\dot{x}_s(t) = \sum_{i=1}^{n} u_i(t)\exp(\mu_i t)v_i^T(0)\dot{x}_s(0).$$

Since $\dot{x}_s(t)$ is periodic, it follows that at least one of the Floquet exponents satisfies $\exp(\mu_i T) = 1.0$. ∎

Remark 5.2: One can show that if 1.0 is a characteristic multiplier and the remaining $n-1$ Floquet exponents satisfy $|\exp(\mu_i T)| < 1.0, \quad i = 2, \cdots, n$, then the periodic solution $x_s(t)$ of (1) is asymptotically orbitally stable and it has the asymptotic phase property (see Appendix A) [23].[6] Moreover, if any of the Floquet exponents satisfy $|\exp(\mu_i T)| > 1.0$, then the solution $x_s(t)$ is orbitally unstable.

Without loss of generality, we choose $\mu_1 = 0$ and $u_1(t) = \dot{x}_s(t)$.

Remark 5.3: With $u_1(t) = \dot{x}_s(t)$ we have $v_1^T(t)\dot{x}_s(t) = 1.0$ and $v_1^T(t)u_j(t) = 0, \quad j = 2, \cdots, n$. $v_1(t)$ will play an important role in the rest of our treatment.

Next, we obtain the particular solution of (3) given by

$$\begin{aligned}w_P(t) &= \int_0^t U(t)\exp(D(t-r))\,V(r)B(x_s(r))b(r)\,dr\\ &= \sum_{i=1}^{n} u_i(t)\int_0^t \exp(\mu_i(t-r))\,v_i^T(r)B(x_s(r))b(r)\,dr.\end{aligned} \tag{6}$$

The first term in the above summation is given by $u_1(t)\int_0^t v_1^T(r)B(x_s(r))b(r)\,dr$ since $\mu_1 = 0$. If the integrand has a nonzero average value, then the deviation $w(t)$ in (3) will grow unbounded, even for small $b(t)$. Hence, the assumption that $w(t)$ is small becomes invalid and the linearized perturbation analysis is inconsistent.

Now, we consider the case where the perturbation $b(t)$ is a vector of uncorrelated white noise sources, i.e.,

$$\mathrm{E}[b(t_1)b^T(t_2)] = I_p\delta(t_1 - t_2) \tag{7}$$

where $\mathrm{E}[.]$ denotes the probabilistic expectation operator. It can be shown that the variance-covariance matrix $K(t) = \mathrm{E}[w(t)w^T(t)]$ of the solution of (3) is given by

$$K(t) = \int_0^t \Phi(t,\,\tau)B(x_s(\tau))B^T(x_s(\tau))\Phi(t,\,\tau)^T\,d\tau$$

[4]By deviation we refer to the difference between the solutions of the perturbed and unperturbed systems.

[5]The reader who is unfamiliar with Floquet theory is encouraged to read Appendix B before continuing.

[6]Note that this is a sufficient condition for asymptotic orbital stability, not a necessary one. We assume that this sufficient condition is satisfied by the system and the periodic solution $x_s(t)$.

for the initial condition $K(0) = 0$. If we substitute $\Phi(t, \tau)$ from (4), we get

$$K(t) = \sum_{i=1}^{n}\sum_{j=1}^{n} u_i(t)u_j^T(t) \cdot \left[\int_0^t \exp((\mu_i+\mu_j)(t-\tau))v_i^T(\tau) \cdot B(x_s(\tau))B^T(x_s(\tau))v_j(\tau)\,d\tau\right].$$

The term in the summation above for $i = j = 1$ is given by

$$u_1(t)u_1^T(t)\left[\int_0^t v_1^T(\tau)B(x_s(\tau))B^T(x_s(\tau))v_1(\tau)\,d\tau\right]$$

since $\mu_1 = 0$. The integrand $v_1^T(\tau)B(x_s(\tau))B^T(x_s(\tau))v_1(\tau)$ (which is a nonnegative[7] scalar that is periodic in τ) has a positive average value, hence, this term grows unbounded with t. Thus, the assumption that the deviation $w(t)$ stays small[8] is also invalid for the stochastic perturbation case because the variances of the entries of $w(t)$ can grow unbounded.

VI. Nonlinear Perturbation Analysis for Phase Deviation

As seen in the previous section, traditional perturbation techniques do not suffice for analyzing oscillators. In this section, a novel nonlinear perturbation analysis suitable for oscillators is presented.

The new analysis proceeds along the following lines.

1) Rewrite (2) with the (small) perturbation $B(x)b(t)$ split into two small parts $b_1(x, t)$ and $\tilde{b}(x, t)$

$$\dot{x} = f(x) + b_1(x, t) + \tilde{b}(x, t). \tag{8}$$

2) Choose the first perturbation term $b_1(x, t)$ in such a way that its effect is to create only phase errors to the unperturbed solution. In other words, show that the equation

$$\dot{x} = f(x) + b_1(x, t) \tag{9}$$

is solved by

$$x_p(t) = x_s(t + \alpha(t)) \tag{10}$$

for a certain function $\alpha(t)$ called the phase deviation. It will be seen that $\alpha(t)$ can grow unboundedly large with time, even though the perturbation $b_1(x, t)$ remains small.

3) Now treat the remaining term $\tilde{b}(x, t)$ as a small perturbation to (9) and perform a consistent traditional perturbation analysis in which the resultant deviations from $x_p(t)$ remain small, i.e., show that

$$z(t) = x_s(t + \alpha(t)) + y(t) \tag{11}$$

solves (8) for a certain $y(t)$ that remains small for all t. $y(t)$ will be called the orbital deviation. Note that we will indeed perform a linearized perturbation analysis for the orbital deviation $y(t)$. However, in this case we prove that this linear analysis is correct and consistent by showing that the orbital deviation indeed stays small for small perturbations. In the traditional linear perturbation analysis presented in Section V, the response deviation for the system does not stay small for small perturbations, hence it is not valid. We also would like to reemphasize that even though the perturbation analysis for the orbital deviation is linear, we derive a nonlinear equation for the phase deviation, hence, we perform a nonlinear perturbation analysis for the overall deviation, i.e., the phase deviation and the orbital deviation.

We start by defining $\alpha(t)$ concretely through a differential equation.

Definition 6.1: Define $\alpha(t)$ by

$$\frac{d\alpha(t)}{dt} = v_1^T(t + \alpha(t))B(x_s(t + \alpha(t)))b(t), \qquad \alpha(0) = 0. \tag{12}$$

Remark 6.1: The existence and uniqueness theorem for differential equations guarantees that $\alpha(t)$ exists and is unique.

Remark 6.2: $\alpha(t)$ can grow unbounded even if $b(t)$ remains small. For example, consider the case where $b(t)$ is a small positive constant $\epsilon \ll 1$, $B \equiv 1$ and $v_1(t)$ is a constant k. Then $\alpha(t) = k\epsilon t$.

Having defined $\alpha(t)$, we are in a position to split $B(x)b(t)$ into $b_1(x, t)$ and $\tilde{b}(x, t)$.

Definition 6.2: Let

$$b_1(x, t) = c_1(x, t)u_1(t + \alpha(t)) \tag{13}$$

and

$$\tilde{b}(x, t) = B(x)b(t) - b_1(x, t) = \sum_{i=2}^{n} c_i(x, t)u_i(t + \alpha(t)) \tag{14}$$

where the scalars $c_i(x, t) = v_i^T(t + \alpha(t))B(x)b(t)$. Note that $b_1(x, t)$ is obtained by projecting the original perturbation along the time-varying direction $u_1(t + \alpha(t))$. u_i, v_i are the Floquet eigenvectors of Section V and Appendix B.

Lemma 6.1: $x_p(t) = x_s(t + \alpha(t))$ solves (9).

Proof: Substituting $x_s(t + \alpha(t))$ in (9) and using $\dot{x}_s(t) = u_1(t)$ we obtain

$$\begin{aligned}&\dot{x}_s(t + \alpha(t))\,(1 + \dot{\alpha}(t))\\ &\quad = f(x_s(t + \alpha(t))) + v_1^T(t + \alpha(t))\\ &\qquad \cdot B(x_s(t + \alpha(t)))b(t)u_1(t + \alpha(t))\\ &\quad \Rightarrow \dot{\alpha}(t)u_1(t + \alpha(t))\\ &\quad = v_1^T(t + \alpha(t))B(x_s(t + \alpha(t)))b(t)u_1(t + \alpha(t)).\end{aligned}$$

Note that $\alpha(t)$ and $c_1(t)$ are scalars, while $u_1(t)$ and $v_1(t)$ are vectors. Also for any t, all the entries of $\dot{x}_s(t)$ and, hence, $u_1(t)$ cannot be simultaneously zero, otherwise the oscillator will cease to oscillate. Hence, $\dot{\alpha}(t) = v_1^T(t + \alpha(t))B(x_s(t + \alpha(t)))b(t)$. ■

[7] $B(x_s(\tau))B^T(x_s(\tau))$ is a positive semidefinite matrix.

[8] The notion of staying small is quite different for a stochastic process than the one for a deterministic function. For instance, a Gaussian random variable can take arbitrarily large values with nonzero probability even when its variance is small. We say that a stochastic process is bounded when its variance is bounded, even though some of its sample paths (representing a nonzero probability) can grow unbounded.

With Lemma 6.1, we have shown that the $b_1(x, t)$ component causes deviations only along the limit cycle, i.e., phase deviations. Next, we show that the remaining perturbation component $\tilde{b}(x, t)$ perturbs $x_p(t)$ only by a small amount $y(t)$, provided $b(t)$ is small.

Lemma 6.2: For $b(t)$ sufficiently small, the mapping $t \mapsto t + \alpha(t)$ is invertible.

Proof: It suffices to show that $\hat{t}(t) = t + \alpha(t)$ is strictly monotonic. The derivative of this function is $1 + \dot{\alpha}(t)$. Now $\dot{\alpha}(t) = v_1^T(t+\alpha(t))B(x_s(t+\alpha(t)))b(t)$. The terms $v_1^T(\cdot)$ and $B(x_s(\cdot))$ are both bounded because they are periodic with t. Hence, $|\dot{\alpha}(t)|$ can be made less than one if $b(t)$ is small enough. Since the derivative of the mapping will then be strictly greater than zero, the mapping $t \mapsto t + \alpha(t)$ will be invertible.

Definition 6.3: Let $b(t)$ be small enough that $\hat{t}(t) = t+\alpha(t)$ is invertible. Then define $\hat{b}(\cdot)$ by

$$\hat{b}(\hat{t}) = b(t). \tag{15}$$

Definition 6.4: Define

$$y(t) = \sum_{i=2}^{n} u_i(\hat{t}) \int_0^{\hat{t}} \exp\big(\mu_i(\hat{t}-r)\big)\, v_i^T(r) B(x_s(r))\hat{b}(r)\, dr \tag{16}$$

where $\hat{t} = t + \alpha(t)$.

Remark 6.3: Note that the index of the summation starts from two. Since $|\exp(\mu_i T)| < 1.0$, $i \geq 2$ (due to asymptotic orbital stability), this implies that $y(t)$ is within a constant factor of $b(t)$, hence, small.

Theorem 6.1: If $b(t)$ is small [implying that $y(t)$ in Definition 6.4 is also small], then $z(t) = x_p(t) + y(t)$ solves (8) to first order in $y(t)$.

Proof: Consider (9) perturbed by $\tilde{b}(x, t)$ to obtain (8). Assume the solution to be $z(t)$. Then we have

$$\begin{aligned}\dot{x}_p(t) + \dot{y}(t) &= f(x_p(t) + y(t)) + b_1(x_p(t) + y(t), t) \\ &\quad + \tilde{b}(x_p(t) + y(t), t) \\ \Rightarrow \dot{y}(t) &\approx \left.\frac{\partial f}{\partial x}\right|_{x_p(t)} y(t) + \tilde{b}(x_p(t), t)\end{aligned}$$

[ignoring higher order terms in $b(t)$ and $y(t)$ and using Lemma 6.1]

$$\Rightarrow \dot{y}(t) \approx A(x_s(t+\alpha(t)))y(t) + \tilde{b}(x_s(t+\alpha(t)), t)$$

with $A(x) = (\partial f/\partial x)|_x$.

Now define $\hat{t}(t) = t + \alpha(t)$ and apply Lemma 6.2 to invert $\hat{t}(t)$ in order to define

$$\hat{y}(\hat{t}) = y(t) \tag{17}$$

$$\hat{b}(x_s(\hat{t}), \hat{t}) = \tilde{b}(x_s(\hat{t}), t). \tag{18}$$

Then we have

$$\begin{aligned}\Rightarrow \frac{d\hat{y}(\hat{t})}{dt} &\approx A(x_s(\hat{t}))\hat{y}(\hat{t}) + \hat{b}(x_s(\hat{t}), \hat{t}) \\ \Rightarrow (1+\dot{\alpha}(t))\frac{d\hat{y}(\hat{t})}{d\hat{t}} &\approx A(x_s(\hat{t}))\hat{y}(\hat{t}) + \hat{b}(x_s(\hat{t}), \hat{t}).\end{aligned}$$

From (12), note that $\dot{\alpha}$ is bounded to within a constant multiple of $b(t)$, hence, $|\dot{\alpha}| \ll 1$ if $|b(t)| \ll 1$. Hence, we can approximate $1 + \dot{\alpha}$ by one to obtain

$$\frac{d\hat{y}(\hat{t})}{d\hat{t}} \approx A(x_s(\hat{t}))\hat{y}(\hat{t}) + \hat{b}(x_s(\hat{t}), \hat{t}). \tag{19}$$

Equation (19) is of the same form as (3), hence, its solution is of the form of (6)

$$\hat{y}(\hat{t}) = \sum_{i=1}^{n} u_i(\hat{t}) \int_0^{\hat{t}} \exp\big(\mu_i(\hat{t}-r)\big)\, v_i^T(r)\hat{b}(x_s(r), r)\, dr. \tag{20}$$

Consider the $i = 1$ term of (20). Since $\mu_1 = 0$, the integrand equals the $v_1^T(r)\hat{b}(x_s(r), r)$. From its definition of $\hat{b}$ in (18) and (14) it is clear that $\hat{b}$, expressed in the basis $\{u_i(\cdot)\}$, contains no u_1 component. Therefore, by biorthogonality of $\{u_i(\cdot)\}$ and $\{v_i(\cdot)\}$, $v_1^T(r)\hat{b}(x_s(r), r)$ is identically zero, hence, the $i = 1$ term vanishes. The expression for $y(t)$ then becomes

$$\begin{aligned}y(t) &= \hat{y}(\hat{t}) \\ &= \sum_{i=2}^{n} u_i(\hat{t}) \int_0^{\hat{t}} \exp\big(\mu_i(\hat{t}-r)\big)\, v_i^T(r)\hat{b}(x_s(r), r)\, dr \\ \Rightarrow y(t) &= \sum_{i=2}^{n} u_i(\hat{t}) \int_0^{\hat{t}} \exp\big(\mu_i(\hat{t}-r)\big) v_i^T(r) B(x_s(r))\hat{b}(r)\, dr.\end{aligned}$$

■

VII. Stochastic Characterization of the Phase Deviation α

We now find the probabilistic characterization of the phase deviation α (Definition 6.1) as a stochastic process when the perturbation $b(t)$ is a vector of uncorrelated[9] white noise sources as in (7). We assume that $b(t)$ is stationary. White cyclostationary (i.e., modulated white) noise sources are captured with the state-dependent modulation $B(x)$ in (2). In this paper, we consider only white and modulated-white noise sources, such as shot and thermal noise. Please see [21] for a treatment of colored and modulated-colored noise sources, such as $1/f$ noise.

We will treat (12) as a stochastic differential equation [25], [26]. The stochastic process α is a family $\{\alpha(t)\colon\ t \in \mathbb{R}_+\}$ of random variables indexed by time t and taking values in $\mathbb{R}$. Evaluation of the random variable $\alpha(t)$ at some time t yields a number in $\mathbb{R}$ and an evaluation of α for all $t \in \mathbb{R}_+$ is called a realization or sample path of the stochastic process α. The complete collection of the sample paths of the stochastic process α is called the ensemble. The $\alpha(t)$ (for different values of t) are not independent, in general. If $\boldsymbol{t} = [t_1, t_2, \cdots, t_n]$ is a vector taking values in $\mathbb{R}_+$, then the vector $[\alpha(t_1), \alpha(t_2), \cdots, \alpha(t_n)]$ has the joint distribution function $F_d(\boldsymbol{\eta}, \boldsymbol{t})\colon \mathbb{R}^n \to [0, 1]$ given by

$$F_d(\boldsymbol{\eta}, \boldsymbol{t}) = \mathrm{P}\left(\alpha(t_1) \leq \eta_1, \cdots, \alpha(t_n) \leq \eta_n\right)$$

[9]The extension to correlated noise sources is trivial. We consider uncorrelated noise sources for notational simplicity. Moreover, various noise sources in electronic devices usually have independent physical origin and, hence, they are modeled as uncorrelated stochastic processes.

where $\mathrm{P}(.)$ denotes the probability measure. The collection $\{F(\boldsymbol{\eta}, \boldsymbol{t})\}$, as $\boldsymbol{t}$ ranges over all vectors of members of $\mathbb{R}_+$ of any finite length, is called the collection of finite-dimensional distributions (FDD's) of α. In general, the knowledge of the FDD's of a process α does not yield complete information about the properties of its sample paths [27]. Nevertheless, the FDD's provide more than adequate information to calculate the second-order (e.g., spectral) properties of a stochastic process, since they capture the correlation information between $\alpha(t_1)$ and $\alpha(t_2)$ for all $t_1, t_2 \in \mathbb{R}_+$.

In this section, we will follow the below procedure to find an adequate probabilistic characterization of the phase deviation α for our purposes.

1) We first calculate the time-varying probability density function (PDF) $p_\alpha(\eta, t)$ of α defined as

$$p_\alpha(\eta, t) = \frac{\partial \mathrm{P}(\alpha(t) \le \eta)}{\partial \eta}, \qquad t \ge 0$$

and show that it becomes the PDF of a Gaussian random variable asymptotically with t. A Gaussian PDF is completely characterized by the mean and the variance of the random variable. We show that $\alpha(t)$ becomes, asymptotically with time, a Gaussian random variable with a constant (as a function of t) mean and a variance that is linearly increasing with time.[10]

2) The time-varying PDF $p_\alpha(\eta, t)$ does not provide any correlation information between $\alpha(t)$ and $\alpha(t+\tau)$ that is needed for the evaluation of its spectral characteristics. We then calculate this correlation to be

$$\mathrm{E}[\alpha(t)\alpha(t+\tau)] = m^2 + c \min(t, t+\tau)$$

where m and c are scalar constants.

3) We then show that $\alpha(t_1)$ and $\alpha(t_2)$ become jointly Gaussian asymptotically with time, which does not follow immediately from the fact that they are individually Gaussian.

Starting with the stochastic differential (12) for α, one can derive (see Appendix C) a partial differential equation, known as the Fokker–Planck equation [26], [28] for the time-varying PDF $p_\alpha(\eta, t)$. The Fokker–Planck equation for $\alpha(t)$ takes the form

$$\frac{\partial p_\alpha(\eta, t)}{\partial t} = -\frac{\partial}{\partial \eta}\left(\lambda p_\alpha(\eta, t)\frac{\partial v^T(t+\eta)}{\partial \eta} v(t+\eta)\right) + \frac{1}{2}\frac{\partial^2}{\partial \eta^2}\left(v^T(t+\eta)v(t+\eta)p_\alpha(\eta, t)\right) \quad (21)$$

where

$$v^T(t) = v_1^T(t) B(x_s(t))$$

and $0 \le \lambda \le 1$ depends on the definition of the stochastic integral [26] used to interpret the stochastic differential equation in (12). We would like to solve (21) for $p_\alpha(\eta, t)$. It turns out that $p_\alpha(\eta, t)$ becomes a Gaussian PDF asymptotically with linearly increasing variance. We show this by first solving for the characteristic function $F(\omega, t)$ of $\alpha(t)$, which is defined by

$$F(\omega, t) = \mathrm{E}[\exp(j\omega\alpha(t))] = \int_{-\infty}^{\infty} \exp(j\omega\eta) p_\alpha(\eta, t)\, d\eta.$$

Since both $v_1^T(.)$ and $B(x_s(.))$ are T periodic in their arguments, $v^T(.)$ is also periodic in its argument with period T. Hence, we can expand $v^T(t)$ into its Fourier series

$$v^T(t) = \sum_{i=-\infty}^{\infty} V_i^T \exp(ji\omega_0 t), \qquad \omega_0 = \frac{2\pi}{T}.$$

Lemma 7.1: The characteristic function of $\alpha(t)$, $F(\omega, t)$, satisfies

$$\frac{\partial F(\omega, t)}{\partial t} = \sum_{i=-\infty}^{\infty}\sum_{k=-\infty}^{\infty} V_i^T V_k^* \exp(j\omega_0(i-k)t) \cdot \left(-\lambda\omega_0 i\omega - \tfrac{1}{2}\omega^2\right) F(\omega_0(i-k)+\omega, t) \quad (22)$$

where $*$ denotes complex conjugation.

Proof: Let $h(\eta)$ be a smooth function. For notational simplicity we will drop the explicit dependence of $p_\alpha(\eta, t)$, $h(\eta)$, and $v^T(t+\eta)$ on η and t from now on. Then from (21) we have

$$\int_{-\infty}^{\infty} \frac{\partial p_\alpha}{\partial t} h\, d\eta = \int_{-\infty}^{\infty} -\frac{\partial}{\partial \eta}\left(\lambda p_\alpha \frac{\partial v^T}{\partial \eta} v\right) h\, d\eta + \int_{-\infty}^{\infty} \frac{1}{2}\frac{\partial^2 (v^T v p_\alpha)}{\partial \eta^2} h\, d\eta.$$

The term on the left-hand side is the time derivative of $\mathrm{E}[h(\alpha(t))] = \int_{-\infty}^{\infty} p_\alpha(\eta, t) h(\eta)\, d\eta$. The first term on the right-hand side is

$$\int_{-\infty}^{\infty} -\frac{\partial}{\partial \eta}\left(\lambda p_\alpha \frac{\partial v^T}{\partial \eta} v\right) h\, d\eta.$$

Integrating this by parts we get

$$\int_{-\infty}^{\infty} -\frac{\partial}{\partial \eta}\left(\lambda p_\alpha \frac{\partial v^T}{\partial \eta} v\right) h\, d\eta = -\lambda p_\alpha \frac{\partial v^T}{\partial \eta} v h \Big|_{-\infty}^{\infty} + \int_{-\infty}^{\infty} \lambda \frac{dh}{d\eta} p_\alpha \frac{\partial v^T}{\partial \eta} v\, d\eta.$$

The first term above, on the right-hand side, is zero at both the limits, because the PDF of a well-defined random variable should be zero at $\pm\infty$. The second term can be written as an expectation, i.e.,

$$\int_{-\infty}^{\infty} \lambda \frac{dh}{d\eta} p_\alpha \frac{\partial v^T}{\partial \eta} v\, d\eta = \mathrm{E}\left[\lambda \frac{dh}{d\alpha}\frac{\partial v^T}{\partial \alpha} v\right].$$

Similarly (using integration by parts twice) it can be shown that

$$\int_{-\infty}^{\infty} \frac{1}{2}\frac{\partial (v^T v p_\alpha)}{\partial \eta^2} h\, d\eta = \frac{1}{2}\mathrm{E}\left[\frac{d^2 h}{d\alpha^2} v^T v\right].$$

Hence

$$\frac{d\mathrm{E}[h]}{dt} = \mathrm{E}\left[\lambda \frac{dh}{d\alpha}\frac{\partial v^T}{\partial \alpha} v\right] + \frac{1}{2}\mathrm{E}\left[\frac{d^2 h}{d\alpha^2} v^T v\right].$$

[10] The fact that $\alpha(t)$ is a Gaussian random variable for every t does not imply that α is a Gaussian stochastic process. α is a Gaussian process if its FDD's are multivariate Gaussian distributions. Individually Gaussian random variables are not necessarily jointly Gaussian. In this step, we only calculate the time-varying PDF of $\alpha(t)$ which is only a partial characterization of its FDD's [27].

We will now substitute $h(\alpha) = \exp(j\omega\alpha)$ and the Fourier series representation of v to obtain a differential equation for the characteristic function. The left-hand side term is the time derivative of the characteristic function $F(\omega, t)$ of $\alpha(t)$

$$\begin{aligned}
&\frac{\partial F(\omega, t)}{\partial t} \\
&\quad = \mathrm{E}\left[j\omega\lambda\frac{\partial v^T}{\partial\alpha}\, v\, \exp(j\omega\alpha) + \frac{1}{2}\,(j\omega)^2 v^T v\, \exp(j\omega\alpha)\right] \\
&\quad = \sum_{i=-\infty}^{\infty}\sum_{k=-\infty}^{\infty} V_i^T V_k^*\, \exp(j\omega_0(i-k)t)\mathrm{E} \\
&\qquad \cdot\left[\left(-\lambda\omega_0 i\omega - \tfrac{1}{2}\,\omega^2\right)\exp(j\omega_0(i-k)\alpha + j\omega\alpha)\right] \\
&\quad = \sum_{i=-\infty}^{\infty}\sum_{k=-\infty}^{\infty} V_i^T V_k^*\, \exp(j\omega_0(i-k)t) \\
&\qquad \cdot\left(-\lambda\omega_0 i\omega - \tfrac{1}{2}\,\omega^2\right) F(\omega_0(i-k)+\omega, t).
\end{aligned}$$

■

Theorem 7.1: (22) has a solution that becomes the characteristic function of a Gaussian random variable asymptotically with time

$$\lim_{t\to\infty} F(\omega, t) = \exp\left(j\omega\mu(t) - \frac{\omega^2\sigma^2(t)}{2}\right) \tag{23}$$

solves (22) where $\mu(t) = m$ is a constant and $\sigma^2(t) = ct$ where

$$c = \frac{1}{T}\int_0^T v^T(t)v(t)\,dt. \tag{24}$$

The variance of this Gaussian random variable increases linearly with time, exactly as in a Wiener process.

Proof: The characteristic function of a Gaussian random variable with mean $\mu(t)$ and variance $\sigma^2(t)$ is given by $\exp(j\omega\mu(t) - 1/2\omega^2\sigma^2(t))$ [27]. Substituting this expression in (22) for the characteristic function we obtain

$$\begin{aligned}
&\left(j\omega\frac{d\mu}{dt} - \frac{\omega^2}{2}\frac{d\sigma^2}{dt}\right)\exp\left(j\omega\mu - \frac{1}{2}\,\omega^2\sigma^2\right) \\
&\quad = \sum_{i=-\infty}^{\infty}\sum_{k=-\infty}^{\infty} V_i^T V_k^*\, \exp(j\omega_0(i-k)t)\left(-\lambda\omega_0 i\omega - \tfrac{1}{2}\,\omega^2\right) \\
&\qquad \cdot\exp(j(\omega+\omega_0(i-k))\mu)\exp\left(-\tfrac{1}{2}(\omega+\omega_0(i-k))^2\sigma^2\right)
\end{aligned}$$

where we dropped the explicit dependence of $\mu(t)$ and $\sigma^2(t)$ on t. Or equivalently

$$\begin{aligned}
&\left(j\omega\frac{d\mu}{dt} - \frac{\omega^2}{2}\frac{d\sigma^2}{dt}\right) \\
&\quad = \sum_{i=-\infty}^{\infty}\sum_{k=-\infty}^{\infty} V_i^T V_k^*\, \exp(j\omega_0(i-k)t)\left(-\lambda\omega_0 i\omega - \tfrac{1}{2}\,\omega^2\right) \\
&\qquad \cdot\exp(j\omega_0(i-k)\mu)\exp(-\omega\omega_0(i-k)\sigma^2) \\
&\qquad \cdot\exp\left(-\tfrac{1}{2}\,\omega_0^2(i-k)^2\sigma^2\right).
\end{aligned} \tag{25}$$

This equation should be valid for all values of ω. Hence, the coefficients of equal powers of ω on both sides should be equal. Expanding $\exp(-\omega\omega_0(i-k)\sigma^2)$ in a power series and equating the coefficients of ω on both sides we obtain

$$\begin{aligned}
j\frac{d\mu}{dt} &= \sum_{i=-\infty}^{\infty}\sum_{k=-\infty}^{\infty} V_i^T V_k^*\, \exp(j\omega_0(i-k)t) \\
&\quad \cdot\exp(j\omega_0(i-k)\mu)\exp\left(-\tfrac{1}{2}\,\omega_0^2(i-k)^2\sigma^2\right)(-\lambda\omega_0 i)
\end{aligned}$$

or

$$\begin{aligned}
\frac{d\mu}{dt} &= \sum_{i=-\infty}^{\infty}\sum_{k=-\infty}^{\infty} j\lambda\omega_0 i V_i^T V_k^*\, \exp(j\omega_0(i-k)t) \\
&\quad \cdot\exp(j\omega_0(i-k)\mu)\exp\left(-\tfrac{1}{2}\,\omega_0^2(i-k)^2\sigma^2\right).
\end{aligned} \tag{26}$$

For large t and, hence, large σ^2, $\exp(-1/2\omega_0^2(i-k)^2\sigma^2)$ becomes vanishingly small for all $i \neq k$. For $i = k$ the above equation becomes

$$\begin{aligned}
\frac{d\mu}{dt} &= \sum_{i=-\infty}^{\infty} j\lambda\omega_0 i V_i^T V_i^* \\
&= \frac{\lambda}{T}\int_0^T \frac{dv^T(t)}{dt}\, v(t)\,dt \\
&= \frac{\lambda}{2T}\int_0^T \frac{dv^T(t)v(t)}{dt}\,dt \\
&= \frac{\lambda}{2T} v^T(t)v(t)\Big|_0^T \\
&= 0
\end{aligned}$$

where we used the fact that $v(t)$ and hence $v^T(t)v(t)$ is T periodic in evaluating the integral. Hence, asymptotically, the mean $\mu(t)$ becomes a constant.

Equating the coefficients of ω^2 on both sides of (25) we obtain

$$\begin{aligned}
\frac{d\sigma^2}{dt} &= \sum_{i=-\infty}^{\infty}\sum_{k=-\infty}^{\infty} (1 - 2\lambda\omega_0^2 i(i-k)\sigma^2) V_i^T V_k^* \\
&\quad \cdot\exp(j\omega_0(i-k)t)\exp(j\omega_0(i-k)\mu) \\
&\quad \cdot\exp\left(-\tfrac{1}{2}\,\omega_0^2(i-k)^2\sigma^2\right).
\end{aligned} \tag{27}$$

Using the same arguments as above we can show that for large t

$$\begin{aligned}
\frac{d\sigma^2}{dt} &= \sum_{i=-\infty}^{\infty} V_i^T V_i^* \\
&= \frac{1}{T}\int_0^T v^T(t)v(t)\,dt = c
\end{aligned}$$

which is the time average of $v^T(t)v(t)$. This shows that, asymptotically, the variance is growing linearly with t and the slope is the time average of $v^T(t)v(t)$. The differential (26) and (27) for $\sigma^2(t)$ and $\mu(t)$ form a pair of coupled differential equations and can be solved numerically to obtain the final value m to which $\mu(t)$ settles.

Now, we examine the coefficients of ω^n in (25) for $n > 2$. Equating the coefficients of ω^n, $n > 2$ on both sides of (25), we obtain

$$0 = \sum_{i=-\infty}^{\infty} \sum_{k=-\infty}^{\infty} \cdot \left(-\lambda\omega_0 i \frac{(-\omega_0(i-k)\sigma^2)^{n-1}}{(n-1)!} - \frac{1}{2}\frac{(-\omega_0(i-k)\sigma^2)^{n-2}}{(n-2)!} \right) \cdot V_i^T V_k^* \exp(j\omega_0(i-k)t)\exp(j\omega_0(i-k)\mu) \cdot \exp\left(-\tfrac{1}{2}\omega_0^2(i-k)^2\sigma^2\right). \quad (28)$$

For large t, $\sigma^2(t)$ becomes large (increasing linearly with t), hence, $\exp(-1/2\omega_0^2(i-k)^2\sigma^2)$ becomes vanishingly small for all $i \neq k$. The term on the right-hand side of the above equation with $i = k$ is identically zero. Hence, (28) becomes consistent asymptotically in time with $\mu(t) = m$ and $\sigma^2(t) = ct$. Now, given the derivation above, it is trivial to show that the characteristic function of the Gaussian distribution with mean $\mu(t) = m$ and variance $\sigma^2(t) = ct$ asymptotically satisfies (22). ■

Remark 7.1: $\alpha(t)$ becomes, asymptotically with t, a Gaussian random variable with mean $\mu(t) = m$ and variance $\sigma^2(t) = ct$.

Lemma 7.2:

$$\mathrm{E}[\alpha(t)\alpha(t+\tau)] = \begin{cases} \mathrm{E}[\alpha^2(t)] & \text{if } \tau \geq 0 \\ \mathrm{E}[\alpha^2(t+\tau)] & \text{if } \tau < 0 \end{cases}.$$

Sketch of Proof: The proof is trivial if we interpret (12) using Ito's definition of the stochastic integral [25] [corresponding to $\lambda = 0$ in (21)] because then, using the integral form of (12) that defines α, one can write for $\tau \geq 0$

$$\alpha(t+\tau) = \alpha(t) + (\alpha(t+\tau) - \alpha(t)) = \alpha(t) + \xi(t, \tau)$$

where $\xi(t, \tau)$ is uncorrelated with $\alpha(t)$. The proof is more involved for the case $0 < \lambda \leq 1$, for which we use the integral form of (12) and the fact that $v^T(t+\alpha(t))$ is bounded for any stochastic process α [29]. ■

Corollary 7.1: Asymptotically with t

$$\mathrm{E}[\alpha(t)\alpha(t+\tau)] = m^2 + c\,\min(t, t+\tau).$$

Proof: Follows trivially from Lemma 7.2 and Remark 7.1. ■

Definition 7.1: Two real valued random variables Ψ_1 and Ψ_2 are called jointly Gaussian if for all $a_1, a_2 \in \mathbb{R}$, the real random variable $a_1\Psi_1 + a_2\Psi_2$ is Gaussian.

Theorem 7.2: Asymptotically with time, $\alpha(t_1)$ and $\alpha(t_2)$ become jointly Gaussian.

Sketch of Proof: The proof is trivial if we interpret (12) using Ito's definition of the stochastic integral [25] [corresponding to $\lambda = 0$ in (21)], as in the proof of Lemma 7.2. The proof is more involved for $0 < \lambda \leq 1$. In this case, we prove this result by showing that the cumulants of $a_1\alpha(t_1) + a_2\alpha(t_2)$ (for any $a_1, a_2 \in \mathbb{R}$) vanish for order higher than two. The cumulants of a random variable Ψ are defined as the coefficients in the Taylor series expansion of its cumulant generating function which is, in turn, defined by

$$K_\psi = \log \mathrm{E}[\exp(\theta\Psi)] = \sum_{i=1}^{\infty} \frac{1}{i!} k_i(\Psi)\theta^i$$

where $k_i(\Psi)$ is the ith-order cumulant [27]. A random variable is Gaussian if and only if its cumulants of order higher than two vanish [26]. In the proof, we also use the fact that $\alpha(t_1)$ and $\alpha(t_2)$ become individually Gaussian asymptotically with t. ■

The stochastic characterization of the phase deviation α we obtained in this section can be summarized by Remark 7.1, Lemma 7.2, Corollary 7.1, and Theorem 7.2. These do not completely specify the FDD's of α as a stochastic process. However, they provide adequate information for a practical characterization of the effect of phase deviation α on the signal generated by an autonomous oscillator, e.g., its spectral properties, as we will see in Sections VIII and IX.

VIII. Spectrum of an Oscillator with Phase Noise

Having obtained the asymptotic stochastic characterization of α, we now compute the PSD of $x_s(t + \alpha(t))$. We first obtain an expression for the nonstationary autocorrelation function $R(t, \tau)$ of $x_s(t + \alpha(t))$. Next, we demonstrate that the autocorrelation becomes independent of t asymptotically. This implies our main result, that the autocorrelation of the oscillator output with phase noise contains no nontrivial cyclostationary components, confirming the intuitive expectation that a noisy autonomous system (with white and modulated-white noise sources in this paper, please see [21] for a generalization of these results to colored noise sources) cannot have periodic cyclostationary variations because it has no perfect time reference. Finally, we show that the PSD of the stationary component is a summation of Lorentzian spectra and that a single scalar constant, namely, c in (24), is sufficient to characterize it.

We start by calculating the autocorrelation function of $x_s(t+\alpha(t))$ given by

$$R(t, \tau) = \mathrm{E}\left[x_s(t+\alpha(t))x_s^*(t+\tau+\alpha(t+\tau))\right]. \quad (29)$$

Definition 8.1: Define X_i to be the Fourier coefficients of $x_s(t)$

$$x_s(t) = \sum_{i=-\infty}^{\infty} X_i \exp(ji\omega_0 t).$$

The following simple Lemma establishes the basic form of the autocorrelation.

Lemma 8.1:

$$R(t, \tau) = \sum_{i=-\infty}^{\infty} \sum_{k=-\infty}^{\infty} X_i X_k^* \exp(j(i-k)\omega_0 t) \cdot \exp(-jk\omega_0\tau)\mathrm{E}\left[\exp(j\omega_0\beta_{ik}(t, \tau))\right] \quad (30)$$

where $\beta_{ik}(t, \tau) = i\alpha(t) - k\alpha(t+\tau)$.

Proof: Follows directly from (29) and Definition 8.1. ■

To evaluate the expectation in the above Lemma, it is useful to consider first the statistics of $\beta_{ik}(t, \tau)$.

Lemma 8.2:

$$\lim_{t\to\infty} \mathrm{E}[\beta_{ik}(t,\tau)] = (i-k)m \tag{31}$$

$$\lim_{t\to\infty} \mathrm{E}\left[(\beta_{ik}(t,\tau))^2\right] - (\mathrm{E}[\beta_{ik}(t,\tau)])^2 = (i-k)^2 ct + k^2 c\tau - 2ikc\min(0,\tau) \tag{32}$$

where m and c are defined in Theorem 7.1.

Also, $\beta_{ik}(t,\tau)$ becomes Gaussian asymptotically with t.

Proof:

$$\begin{aligned}\lim_{t\to\infty} \mathrm{E}[\beta_{ik}(t,\tau)] &= i \lim_{t\to\infty} \mathrm{E}[\alpha(t)] - k \lim_{t\to\infty} \mathrm{E}[\alpha(t+\tau)] \\ &= (i-k)m \text{ (from Remark 7.1)}\end{aligned}$$

$$\begin{aligned}&\lim_{t\to\infty} \mathrm{E}\left[\beta_{ik}^2(t,\tau)\right] \\ &= i^2 \lim_{t\to\infty} \mathrm{E}\left[\alpha^2(t)\right] + k^2 \lim_{t\to\infty} \mathrm{E}\left[\alpha^2(t+\tau)\right] \\ &\quad - 2ik \lim_{t\to\infty} \mathrm{E}[\alpha(t)\alpha(t+\tau)] \\ &= i^2\left(m^2+ct\right) + k^2\left(m^2+c(t+\tau)\right) \\ &\quad - 2ik\left(m^2 + c\min(t, t+\tau)\right) \\ &\quad \text{(using Corollary 7.1)} \\ &= (i-k)^2\left(m^2+ct\right) + k^2c\tau - 2ikc\min(0,\tau)\end{aligned}$$

$$\begin{aligned}&\Rightarrow \lim_{t\to\infty} \mathrm{E}\left[(\beta_{ik}(t,\tau))^2\right] - (\mathrm{E}[\beta_{ik}(t,\tau)])^2 \\ &\quad = (i-k)^2 ct + k^2 c\tau - 2ikc\min(0,\tau).\end{aligned}$$

The asymptotic Gaussianness of $\beta_{ik}(t,\tau)$ follows directly from Theorem 7.2. ∎

Using the asymptotically Gaussian nature of $\beta_{ik}(t,\tau)$, we are now able to obtain a form for the expectation in (30).

Lemma 8.3: If $c > 0$, the characteristic function of $\beta_{ik}(t,\tau)$ is asymptotically independent of t and has the following form:

$$\lim_{t\to\infty} \mathrm{E}[\exp(j\omega_0\beta_{ik}(t,\tau))] = \begin{cases} 0, & \text{if } i \neq k \\ \exp(-\frac{1}{2}\omega_0^2 k^2 c|\tau|), & \text{if } i = k \end{cases}. \tag{33}$$

Proof:

$$\begin{aligned}&\lim_{t\to\infty} \mathrm{E}[\exp(j\omega_0\beta_{ik}(t,\tau))] \\ &\quad = \exp(j\omega_0(i-k)m) \\ &\qquad \cdot \exp(-\tfrac{1}{2}\omega_0^2((i-k)^2ct + k^2c\tau - 2ikc\min(0,\tau)))\end{aligned}$$

using Lemma 8.2 and the form of the characteristic function of a Gaussian random variable [27]. The result follows immediately from the asymptotic limits of this expression. ∎

Lemma 8.4:

$$\lim_{t\to\infty} R(t,\tau) = \sum_{i=-\infty}^{\infty} X_i X_i^* \exp(-ji\omega_0\tau) \cdot \exp(-\tfrac{1}{2}\omega_0^2 i^2 c|\tau|). \tag{34}$$

Proof: The result is obtained by substituting (33) in (30). ∎

The PSD (spectrum) of $x_s(t+\alpha(t))$ can now be determined as follows.

Lemma 8.5: The spectrum of $x_s(t+\alpha(t))$ is determined by the asymptotic behavior of $R(t,\tau)$ as $t \to \infty$. All nontrivial cyclostationary components are zero, while the stationary component of the spectrum is given by

$$S(\omega) = \sum_{i=-\infty}^{\infty} X_i X_i^* \frac{\omega_0^2 i^2 c}{\frac{1}{4}\omega_0^4 i^4 c^2 + (\omega + i\omega_0)^2}. \tag{35}$$

There is also a term $X_0X_0^*\delta(\omega)$ due to the dc part of $x_s(t)$, which is omitted in (35).

Proof: It can be shown [29] that the cyclostationary component [30] of the autocorrelation at any frequency ω_{cyc} is given by

$$R_{\omega_{cyc}}(\tau) = \lim_{T\to\infty} \frac{1}{T}\int_0^T R(t,\tau)\exp(j\omega_{cyc}t)\,dt.$$

This expression is determined by the asymptotic form of $R(t,\tau)$ as a function of t, given in (34). Because this becomes independent of t, the above limit is identically zero for all $\omega_{cyc} \neq 0$, whereas for $\omega_{cyc} = 0$ (the stationary component), it reduces to (34). The result is obtained by taking the Fourier transform of (34). ∎

IX. Phase Noise/Timing Jitter Characterization for Oscillator Design

In this section, we discuss several popular characterizations of phase noise that is used in the design of electronic oscillators and how they can easily be obtained from the stochastic characterization we obtained in Sections VII and VIII.

A. Single-Sided Spectral Density and Total Power

The PSD $S(\omega)$ in (35) (defined for $-\infty < \omega < \infty$, hence, called a double-sided density) is a real and even function of ω because the periodic steady state $x_s(t)$ is real, hence, its Fourier series coefficients X_i in Definition 8.1 satisfy $X_i = X_{-i}^*$. The single-sided spectral density (defined for $0 \le f < \infty$) is given by

$$S_{ss}(f) = 2S(2\pi f) = 2\sum_{i=-\infty}^{\infty} X_i X_i^* \frac{f_0^2 i^2 c}{\pi^2 f_0^4 i^4 c^2 + (f + if_0)^2} \tag{36}$$

where we substituted $\omega = 2\pi f$ and $\omega_0 = 2\pi f_0$. The total power (i.e. the integral of the PSD over the range of the frequencies it is defined for) in $S_{ss}(f)$ is the same as in $S(2\pi f)$, which is

$$\begin{aligned}P_{tot} &= \text{Total power in } S_{ss}(f) \\ &= \int_0^\infty S_{ss}(f)\,df \\ &= \sum_{i=1}^{\infty} 2|X_i|^2.\end{aligned} \tag{37}$$

Note that the total power in the periodic signal $x_s(t)$ (without phase noise) is also equal to the expression in (37) (excluding the power in the dc part), as can be easily seen from the Fourier expansion in Definition 8.1.

Remark 9.1: The phase deviation $\alpha(t)$ does not change the total power in the periodic signal $x_s(t)$, but it alters the power

density in frequency, i.e., the PSD. For the perfect periodic signal $x_s(t)$, the PSD has δ functions located at discrete frequencies (i.e., the harmonics). The phase deviation $\alpha(t)$ spreads the power in these δ functions in the form given in (36), which can be experimentally observed with a spectrum analyzer.

B. Spectrum in dBm/Hz

For electrical oscillators, the state variable in the oscillator that is observed as the output is usually a voltage or a current. The spectrum in (36) is expressed as a function of frequency (f in Hz), then the PSD is in units of volts^2/Hz and amps^2/Hz for a voltage and a current state variable, respectively. Then, the spectral density of the expected (i.e., average, assuming that the stochastic process $x_s(t+\alpha(t)$ is ergodic [30]) power dissipated in a $1\ \Omega$ resistor [with the voltage (current) output of the oscillator as the voltage across (current through) the resistor] is equal to the PSD in (36) (in watts/Hz), which is usually expressed in dBw/Hz as defined by

$$S_{\mathrm{dBw}}(f) = 10\ \log_{10}\left(S_{ss}(f) \text{ in watts/Hz}\right). \tag{38}$$

If $S_{ss}(f)$ is in miliwatts/Hz, then the PSD in dBm/Hz is given by

$$S_{\mathrm{dBm}}(f) = 10\ \log_{10}\left(S_{ss}(f) \text{ in miliwatts/Hz}\right). \tag{39}$$

C. Single-Sideband Phase Noise Spectrum in dBc/Hz

In practice, we are usually interested in the PSD around the first harmonic, i.e., $S_{ss}(f)$ for f around f_0. The single-sideband phase noise $\mathcal{L}(f_m)$ (in dBc/Hz) that is very widely used in practice is defined as

$$\mathcal{L}(f_m) = 10\ \log_{10}\left(\frac{S_{ss}(f_o+f_m)}{2|X_1|^2}\right). \tag{40}$$

For small values of c and for $0 \le f_m \ll f_0$, (40) can be approximated as

$$\mathcal{L}(f_m) \approx 10\ \log_{10}\left(\frac{f_0^2 c}{\pi^2 f_0^4 c^2 + f_m^2}\right). \tag{41}$$

Furthermore, for $\pi f_0^2 c \ll f_m \ll f_0$, $\mathcal{L}(f_m)$ can be approximated by

$$\mathcal{L}(f_m) \approx 10\ \log_{10}\left(\left(\frac{f_0}{f_m}\right)^2 c\right). \tag{42}$$

Notice that the approximation of $\mathcal{L}(f_m)$ in (42) blows up as $f_m \to 0$. For $0 \le f_m < \pi f_0^2 c$, (42) is not accurate, in which case the approximation in (41) should be used.

D. Timing Jitter

In some applications, such as clock generation and recovery, one is interested in a characterization of the phase/time deviation $\alpha(t)$ itself rather than the spectrum of $x_s(t+\alpha(t))$ that was calculated in Section VIII. In these applications, an oscillator generates a square-wave like waveform to be used as a clock. The effect of the phase deviation $\alpha(t)$ on such a waveform is to create deviations or jitter in the zero-crossing or transition times. In Section VII, we found out that $\alpha(t)$ (for an autonomous oscillator) becomes a Gaussian random variable with a linearly increasing variance

$$\sigma^2(t) = ct.$$

Let us take one of the transitions (i.e., edges) of a clock signal as a reference (i.e., trigger) transition and synchronize it with $t = 0$. If the clock signal is perfectly periodic, then one will see transitions exactly at $t_k = kT$, $k = 1, 2, \cdots$ where T is the period. For a clock signal with a phase deviation $\alpha(t)$ that has a linearly increasing variance as above, the timing of the kth transition t_k will have a variance (i.e., mean-square error)

$$\mathrm{E}[(t_k - k\ T)^2] = ckT. \tag{43}$$

The spectral dispersion caused by $\alpha(t)$ in an oscillation signal can be observed with a spectrum analyzer. Similarly, one can observe the timing jitter caused by $\alpha(t)$ using a sampling oscilloscope. McNeill in [12] experimentally observed the linearly increasing variance for the timing of the transitions of a clock signal generated by an autonomous oscillator, as predicted by our theory. Moreover, c (in s^2.Hz) in (43) exactly quantifies the rate of increase of timing jitter with respect to a reference transition. Another useful figure of merit is the cycle-to-cycle timing jitter, i.e., the timing jitter in one clock cycle, which has a variance cT.

E. Noise Source Contributions

The scalar constant c appears in all of the characterizations we discussed above. It is given by

$$c = \frac{1}{T}\int_0^T v_1^T(\tau) B(x_s(\tau)) B^T(x_s(\tau)) v_1(\tau)\, d\tau \tag{44}$$

where $B(.)$: $\mathbb{R}^n \to \mathbb{R}^{n\times p}$ represents the *modulation* of the intensities of the noise sources with the large-signal state. (44) can be rewritten as

$$c = \sum_{i=1}^{p} \frac{1}{T}\int_0^T \left[v_1^T(\tau) B_i(\tau)\right]^2 d\tau = \sum_{i=1}^{p} c_i \tag{45}$$

where p is the number of the noise sources, i.e., the column dimension of $B(x_s(.))$ and $B_i(.)$ is the ith column of $B(x_s(.))$ which maps the ith noise source to the equations of the system. Hence

$$c_i = \frac{1}{T}\int_0^T \left[v_1^T(\tau) B_i(\tau)\right]^2 d\tau \tag{46}$$

represents the contribution of the ith noise source to c. Thus, the ratio

$$\frac{c_i}{c = \sum_{i=1}^{p} c_i} \tag{47}$$

can be used as a figure of merit representing the contribution of the ith noise source to phase noise/timing jitter.

F. Phase Noise Sensitivity

One can also define

$$c_s^{(k)} = \frac{1}{T}\int_0^T \left[v_1^T(\tau) e_k\right]^2 d\tau \tag{48}$$

(where $1 \leq k \leq n$ and e_k is the kth unit vector) as the phase noise/timing jitter sensitivity of the kth equation (i.e., node), because e_k represents a unit intensity noise source added to the kth equation (i.e., connected to the kth node) in (1).

X. Numerical Methods for Phase Noise Characterization

From Sections VII, VIII and IX, for various phase noise characterizations of an oscillator, one needs to calculate the steady-state periodic solution $x_s(t)$ and the periodic vector $v_1(t)$ in (44). Without providing details, we will present outlines of two methods for computing the periodic vector $v_1(t)$: a time-domain one in Section X-A and a frequency-domain one in Section X-B. The latter method is well suited for large circuits.

A. Time Domain Numerical Technique for $v_1(t)$

The procedure for calculating $v_1(t)$ in the time domain is as follows.

1) Compute the large-signal periodic steady-state solution $x_s(t)$ for $0 \leq t \leq T$ by numerically integrating (1), possibly using a technique such as the shooting method [31].
2) Compute the state-transition matrix $\Phi(T, 0)$ (see Appendix B) by numerically integrating

$$\dot{Y} = A(t)Y, \quad Y(0) = I_n$$

from 0 to T, where the Jacobian $A(t)$ is defined in (3). Note that

$$\Phi(T, 0) = Y(T).$$

3) Compute $u_1(0)$ using

$$u_1(0) = \dot{x}_s(0).$$

Note that $u_1(0)$ is an eigenvector of $\Phi(T, 0)$ corresponding to the eigenvalue 1 (see Remark B.3).
4) $v_1(0)$ is an eigenvector of $\Phi^T(T, 0)$ corresponding to the eigenvalue 1 (see Remark B.3). To compute $v_1(0)$, first compute an eigenvector of $\Phi^T(T, 0)$ corresponding to the eigenvalue 1, then scale this eigenvector so that

$$v_1(0)^T u_1(0) = 1 \tag{49}$$

is satisfied.
5) Compute the periodic vector $v_1(t)$ for $0 \leq t \leq T$ by numerically solving the adjoint system

$$\dot{y} = -A^T(t)y \tag{50}$$

using $v_1(0) = v_1(T)$ as the initial condition. Note that $v_1(t)$ is a periodic steady-state solution of (50) corresponding to the Floquet exponent that is equal to zero, i.e., $\mu_1 = 0$ (see Remark B.3). It is not possible to calculate $v_1(t)$ by numerically integrating (50) forward in time because the numerical errors in computing the solution and the numerical errors in the initial condition $v_1(0)$ will excite the modes of the solution of (50) that grow without bound (see Remark B.3). However, one can integrate (50) backward in time with the initial condition $v_1(T) = v_1(0)$ to calculate $v_1(t)$ for $0 \leq t \leq T$ in a numerically stable way.
6) Then, c is calculated using (44).

We implemented the above algorithm in SPICE. We will not present a detailed description of this implementation here, but we will mention a few important points. In implementing the above algorithm, one can increase the efficiency by saving LU factored matrices that needs to be calculated in Step 2 and reuse them in Step 5. If the periodic steady state $x_s(t)$ of the oscillator is calculated using the shooting method [31] in Step 1, then the state transition matrix $\Phi(T, 0)$ of the linear time-varying system obtained by linearizing the nonlinear oscillator circuit around the periodic steady state is already available. It can be shown that the Jacobian of the nonlinear system of equations that is solved in the shooting method (using Newton's method, to calculate the initial condition that results in the periodic steady-state solution) is equal to $\Phi(T, 0) - I$ [32], [33]. Moreover, one can avoid calculating $\Phi(T, 0)$ explicitly and use iterative methods both for the shooting method and at Step 4 to calculate the eigenvector of $\Phi^T(T, 0)$ that corresponds to the eigenvalue 1 [34]. For high-Q oscillators, the iterative methods can run into problems, because $\Phi(T, 0)$ may have several other eigenvalues which are close to 1. In our implementation in SPICE, we explicitly calculate $\Phi(T, 0)$ and perform a full eigenvalue/eigenvector calculation, which allows us to investigate the properties of the state-transition matrix for various oscillator circuits. Even with a full eigenvalue/eigenvector calculation for $\Phi(T, 0)$, the phase noise characterization algorithm discussed above is still very efficient. The phase noise characterization comes almost for free once the periodic steady-state solution $x_s(t)$ is computed.

B. Frequency-Domain Technique for Calculating $v_1(t)$ Using Efficient Harmonic Balance

Definition 10.1: Define the matrices U_i and V_i to be the Fourier components of $U(t)$ and $V(t)$, i.e.,

$$U(t) = \sum_{i=-\infty}^{\infty} U_i e^{j\omega_0 it} \tag{51}$$

$$V(t) = \sum_{i=-\infty}^{\infty} V_i e^{j\omega_0 it}. \tag{52}$$

Definition 10.2: Define the block-Toeplitz matrices $\mathcal{U}$ and $\mathcal{V}$ as follows:

$$\mathcal{U} = \begin{pmatrix} U_0 & U_1 & U_2 & \cdot & \cdot \\ U_{-1} & U_0 & U_1 & U_2 & \cdot \\ U_{-2} & U_{-1} & U_0 & U_1 & U_2 \\ \cdot & U_{-2} & U_{-1} & U_0 & U_1 \\ \cdot & \cdot & U_{-2} & U_{-1} & U_0 \end{pmatrix} \tag{53}$$

$$\mathcal{V} \begin{pmatrix} V_0 & V_1 & V_3 & \cdot & \cdot \\ V_{-1} & V_0 & V_1 & V_2 & \cdot \\ V_{-2} & V_{-1} & V_0 & V_1 & V_2 \\ \cdot & V_{-2} & V_{-1} & V_0 & V_1 \\ \cdot & \cdot & V_{-2} & V_{-1} & V_0 \end{pmatrix}. \tag{54}$$

Lemma 10.1: $\mathcal{U}$ and $\mathcal{V}$ are both invertible since

$$\mathcal{U}\mathcal{V} = \begin{pmatrix} \ddots & & & & & & \\ & I & & & & & \\ & & I & & & & \\ & & & I & & & \\ & & & & I & & \\ & & & & & I & \\ & & & & & & \ddots \end{pmatrix}.$$

Sketch of Proof: Follows from the biorthonormality of $U(t)$ and $V(t)$. ■

Definition 10.3: Define

$$D_k(\omega) = \begin{bmatrix} j(\omega + k\omega_0) - \mu_0 & & \\ & \ddots & \\ & & j(\omega + k\omega_0) - \mu_n \end{bmatrix}.$$

Note D_k is strictly diagonal.

Remark 10.1: Note that $D_k(\omega)$ is singular for $\omega = -k\omega_0$, if the oscillator is asymptotically orbitally stable.

Definition 10.4: Define

$$\mathcal{D}(\omega) = \begin{pmatrix} \ddots & & & & & & \\ & D_2(\omega) & & & & & \\ & & D_1(\omega) & & & & \\ & & & D_0(\omega) & & & \\ & & & & D_{-1}(\omega) & & \\ & & & & & D_{-2}(\omega) & \\ & & & & & & \ddots \end{pmatrix}.$$

Note $\mathcal{D}$ is strictly diagonal.

Remark 10.1: Note that $\mathcal{D}(\omega)$ is singular for $\omega = k\omega_0$, k integer, if the oscillator is asymptotically orbitally stable.

Theorem 10.1: The frequency-domain conversion matrix $\mathcal{H}(\omega)$ of the oscillator [35] is related to $\mathcal{U}$, $\mathcal{D}(\omega)$ and $\mathcal{V}$ by

$$\mathcal{H}(\omega) = \mathcal{U}\mathcal{D}^{-1}(\omega)\mathcal{V}.$$

Theorem 10.2: $\mathcal{H}^{-1}(0)$ is a singular matrix (with rank-deficiency one) and the null space of its transpose is spanned by the Fourier components of $v_1(t)$, i.e.,

$$\begin{aligned} &\ker\left(\mathcal{H}^{-T}(0)\right) \\ &\quad = [1 \quad 0 \quad \cdots \quad 0] \\ &\qquad \cdot [\cdots \quad V_{-2} \quad V_{-1} \quad V_0 \quad V_1 \quad V_2 \quad \cdots] \\ &\quad = [\cdots \quad V_{1,-2}^T \quad V_{1,-1}^T \quad V_{1,0}^T \quad V_{1,1}^T \quad V_{1,2}^T \quad \cdots] \end{aligned} \tag{55}$$

where $V_{1,i}$ are the Fourier coefficients of $kv_1^T(t)$ for some nonzero scalar k, i.e., $kv_1^T(t) = \sum_{i=-\infty}^{\infty} V_{1,i}^T e^{j\omega_0 it}$.

$\mathcal{H}^{-T}(0)$ is simply the transpose of the harmonic balance Jacobian matrix of the oscillator at solution. Its null space can be found efficiently, even for large circuits, by using iterative linear algebra techniques [35]. Hence, a scaled version of $v_1^T(t)$ can be found easily. The scaling constant k can be found by applying $v_1^T(t)u_1(t) = 1$, $u_1(t)$ having first been obtained by differentiating the large-signal steady state solution of the oscillator.

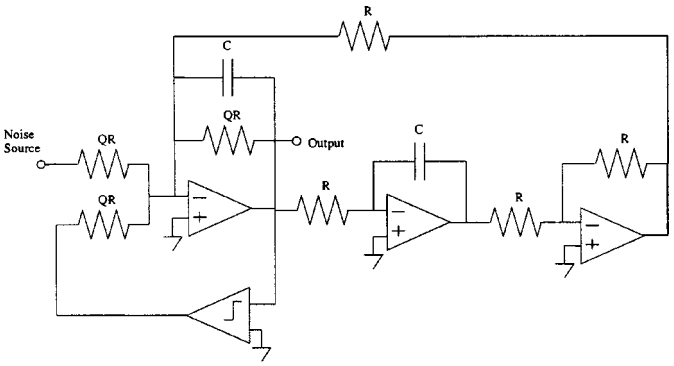

Fig. 4. Oscillator with a bandpass filter and a comparator [36].

XI. Examples

We now present examples for phase noise characterization of practical electronic oscillators.

A. Generic Oscillator with a Bandpass Filter and a Nonlinearity [36]

This oscillator (Fig. 4) consists of a Tow–Thomas second-order bandpass filter and a comparator [36]. If the op amps are considered to be ideal, it can be shown that this oscillator is equivalent (in the sense of the differential equations that describe it) to a parallel RLC circuit in parallel with a nonlinear voltage-controlled current source (or equivalently a series RLC circuit in series with a nonlinear current-controlled voltage source) as in Fig. 1(a). In [36], the authors breadboarded this circuit with an external white noise source (intensity of which was chosen such that its effect is much larger than the other internal noise sources) and measured the PSD of the output with a spectrum analyzer. For $Q = 1$ and $f_o = 6.66$ kHz, we performed a phase noise characterization of this oscillator using the numerical methods in Section X and computed the periodic oscillation waveform $x_s(t)$ for the output and $c = 7.56 \times 10^{-8}$ s^2 Hz. Fig. 5(a) shows the PSD of the oscillator output computed using (36), and Fig. 5(b) shows the spectrum analyzer measurement.[11] Fig. 5(c) shows a blown up version of the PSD around the first harmonic. The single-sideband phase noise spectrum using both (41) and (42) is in Fig. 5(d). Note that (42) cannot predict the PSD accurately below the cut-off frequency $f_c = \pi f_0^2 c = 10.56$ Hz [marked with a $*$ in Fig. 5(d)] of the Lorentzian. The oscillator model that was simulated has two state variables and a single stationary noise source. Fig. 5(e) shows a plot of the periodic nonnegative scalar

$$v_1^T(t)B(x_s(t))B^T(x_s(t))v_1(t) = \left(v_1^T(t)B\right)^2$$

where 2×1 B is independent of t since the noise source is stationary. Recall from (44) that c is the time average of this scalar that is periodic in time.

c can also be obtained relatively accurately in this case using Monte Carlo analysis. We simulated the circuit with 10 000 random excitations and averaged the results to obtain the mean-square difference between the perturbed and unperturbed

[11]The PSD's are plotted in units of dBm as in (39).

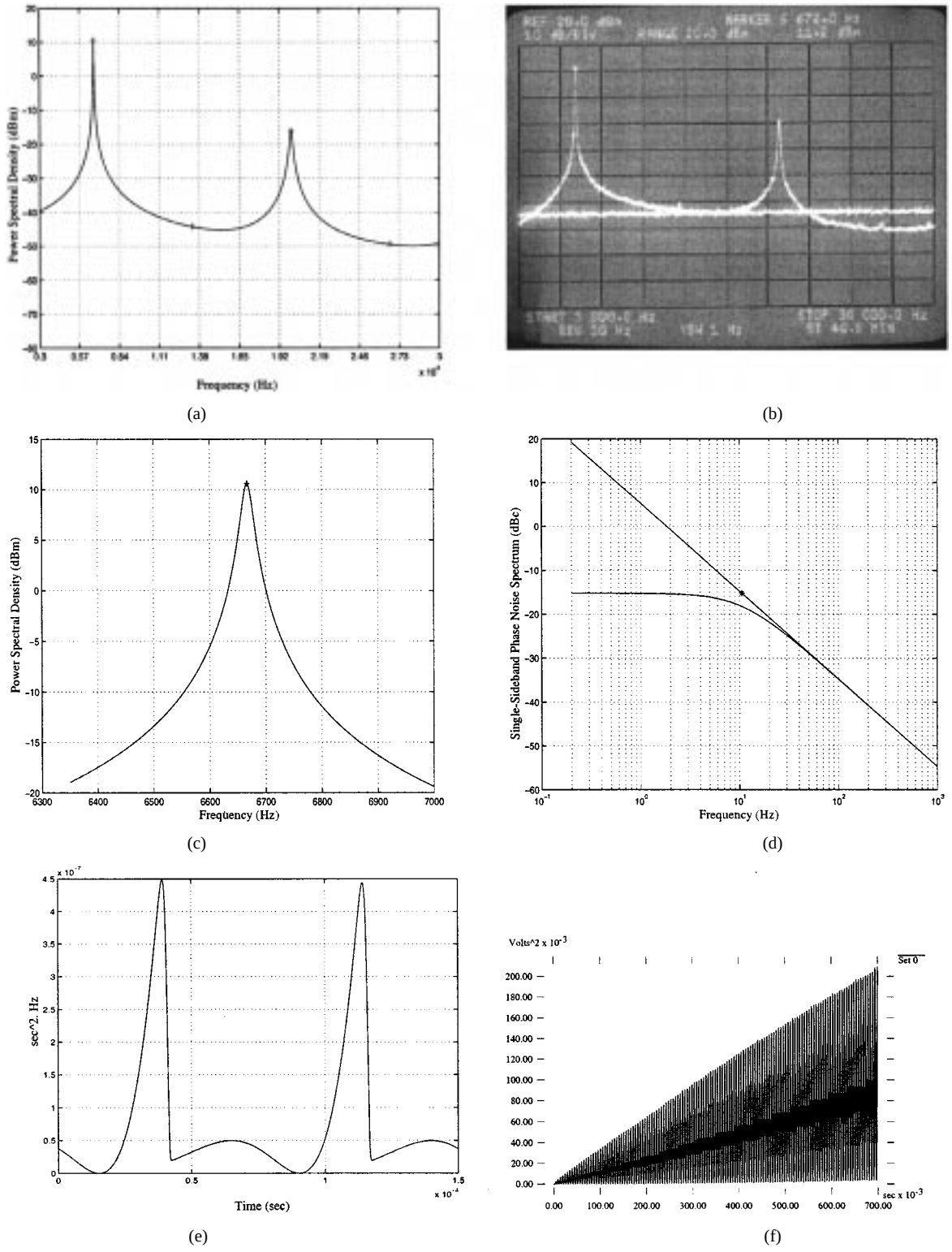

Fig. 5. Phase noise characterization for the oscillator in Fig. 4 (a) Computed PSD (four harmonics). (b) Spectrum analyzer measured PSD [36]. (c) Computed PSD (first harmonic). (d) $\mathcal{L}(f_m)$ computed with both (41) and (42). (e) $(v_1^T(t)B)^2$. (f) Variance of total deviation (Monte Carlo method).

systems as a function of time. Fig. 5(f) illustrates the result, the slope of the envelope of which determines c. The Monte Carlo simulations required small time steps to produce accurate results, since numerical integration methods easily lose accuracy for autonomous circuits. The total computation time for Monte Carlo was about 10 h on a fast SGI workstation (R2000 CPU), whereas our new method required about 20 s: a speedup of more than three orders of magnitude.

B. Ring Oscillator

The ring oscillator circuit is a three-stage oscillator with fully differential ECL buffer delay cells (differential pairs followed

R_c (Ω)	r_b (Ω)	I_{EE} (μA)	f_o (MHz)	c ($\sec^2.\text{Hz} \times 10^{-15}$)
500	58	331	167.7	0.269
2000	58	331	74	0.149
500	1650	331	94.6	0.686
500	58	450	169.5	0.182
500	58	600	169.7	0.151
500	58	715	167.7	0.142

(a)

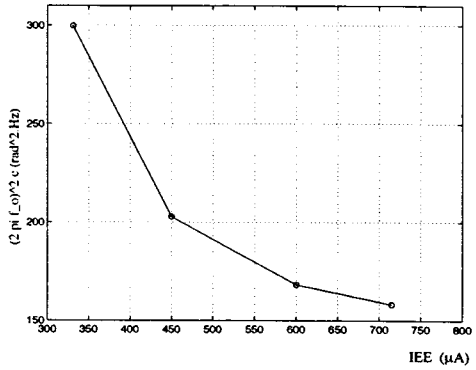

(b)

Fig. 6. Ring-oscillator. (a) Phase noise characterization. (b) Phase noise performance versus I_{EE}.

by emitter followers). This circuit is from [12]. [12] and [11] use analytical techniques to characterize the timing jitter/phase noise performance of ring oscillators with ECL-type delay cells. [12] does the analysis for a bipolar ring oscillator and [11] does it for a CMOS one. Since they use analytical techniques, they use a simplified model of the circuit and make several approximations in their analysis. References [12] and [11] use time-domain Monte Carlo noise simulations to verify the results of their analytical results. They obtain qualitative and some quantitative results and offer guidelines for the design of low phase noise ring oscillators with ECL-type delay cells. However, their results are only valid for their specific oscillator circuits. We will compare their results with the results we will obtain for the above ring oscillator, using the general phase noise characterization methodology we have proposed, which makes it possible to analyze a complicated oscillator circuit without simplifications. We performed several phase noise characterizations of the bipolar ring oscillator. The results are shown in Fig. 6(a) where R_c is the collector load resistance for the differential pair (DP) in the delay cell, r_b is the zero bias base resistance for the BJT's in the DP, I_{EE} is the tail bias current for the DP, and f_o is the oscillation frequency for the three stage ring-oscillator. Note that the changes in R_c and r_b affect the oscillation frequency, unlike the changes in I_{EE}. Fig. 6(b) shows a plot of $(2\pi f_o)^2 c$ versus I_{EE} using the data from Fig. 6(a). This prediction of the dependence of phase noise/timing jitter performance on the tail bias current is in agreement with the analysis and experimental results presented in [12] and [11] for ring oscillators with ECL-type delay cells. Note that larger values for $(2\pi f_o)^2 c$ indicate worse phase noise performance.

Noise sources of	$\frac{c_j}{c=\sum_{i=1}^{p} c_i} \times 100$
M1 and M2	44 %
M3, M4 and M5	16 %
Inductor losses	31 %
Others	9 %

(a)

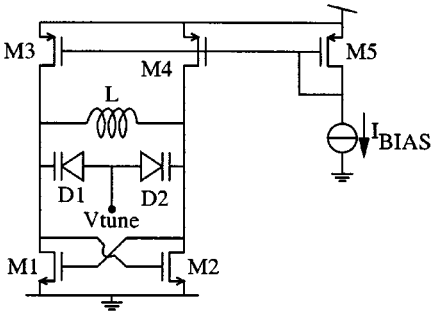

(b)

Fig. 7. Oscillator with on-chip inductor. (a) Noise source contributions. (b) Simplified schematic.

C. Relaxation Oscillator

The relaxation oscillator is a VCO that is based on the emitter-coupled multivibrator circuit [37]. Reference [13] analyzes the process of jitter production for this circuit by describing the circuit behavior with a single first-order stochastic differential equation based on a simplified model for the circuit, and lumping all of the noise sources into a single stationary current noise source. [13] arrives at intuitive qualitative results for low jitter relaxation oscillator design. A relaxation oscillator operates in a highly nonlinear fashion due to regenerative switchings. The analysis of the process of jitter production is not analytically tractable without reverting to simplifications.

For this oscillator, using the numerical methods described in Section X, we obtain

$$f_o = 0.88 \text{ MHz } (2\pi f_o)^2 c = 0.37 \text{rad}^2.\text{Hz}$$

which corresponds to

$$\frac{\sqrt{cT}}{T} = 103.2 \text{ ppm RMS}$$

cycle-to-cycle timing jitter, where ppm is parts per million and RMS is root mean square.

D. Harmonic (Colpitts) Oscillator

The harmonic oscillator has an LC tank, several inductors and a single bipolar-junction transistor with a Colpitts feedback circuit around it. The oscillation frequency is $f_o = 773.2$ MHz. For this oscillator, we computed $(2\pi f_o)^2 c = 1.25$ rad^2.Hz, which corresponds to $\mathcal{L}(f_m) = -115$ dBc/Hz at $f_m = 100$ KHz using (42).

E. 2.5-GHz Oscillator with On-Chip Inductor [38]

A simplified schematic for this oscillator is in Fig. 7(b). We computed $c = 7.16 \times 10^{-20}$ s^2.Hz which corresponds to $\mathcal{L}(f_m) = -103$ dBc/Hz at $f_m = 100$ KHz using (42). There

were 35 state variables and 45 noise sources in the simulated circuit. We generated a noise source contribution report for this oscillator using (47), which is shown in Fig. 7(a).

XII. Conclusions

A novel rigorous theory for phase noise that is valid for any oscillator, regardless of operating mechanism, has been presented. We established novel results about the dynamics of stable nonlinear oscillators in the presence of perturbations, both deterministic and random. An exact nonlinear equation for phase error was derived, which was solved without approximations for random perturbations. This lead us to a precise characterization of timing jitter and spectral dispersion, for computing which we developed efficient numerical methods. We demonstrated our techniques on a variety of practical electrical oscillators and obtained good matches with measurements, even at frequencies close to the carrier, where previous techniques break down. Our methods are more than three orders of magnitude faster than the brute force Monte Carlo approach, which is the only previously available technique that can predict phase noise correctly.

Appendix A
Orbital Stability [23]

If $x_s(t)$ is a nonconstant T-periodic solution of the autonomous system

$$\dot{x} = f(x) \tag{56}$$

then $x_s(t - t_0)$ is also a nonconstant T-periodic solution for arbitrary $t_0 \in \mathbb{R}$. The initial values $x_s(0)$ and $x_s(-t_0)$ can be arbitrarily close (if $|t_0|$ is small enough), and still $x_s(t) - x_s(t - t_0)$ does not tend to zero as t tends to infinity. Let the path γ of the T-periodic solution $x_s(t)$ be

$$\gamma := \{x \in \mathbb{R}: x = x_s(t), \quad t \in \mathbb{R}_+\}.$$

Note that $x_s(t)$ and $x_s(t - t_0)$ have the same path γ.

Definition A.1 (Orbital Stability): The solution $x_s(t)$ of (56) is said to be orbitally stable if for every $\epsilon > 0$ there exists a $\delta(\epsilon)$ such that if the distance of the initial value $x(0) = x_0$ from the path γ of $x_s(t)$ is less than $\delta(\epsilon)$, i.e., $\text{dist}(x_0, \gamma) < \delta(\epsilon)$, then the solution $\phi(t, x_0)$ of (56) that assumes the value x_0 at $t = 0$ satisfies

$$\text{dist}(\phi(t, x_0), \gamma) < \epsilon$$

for $t \geq 0$.

If the solution $x_s(t)$ is orbitally stable, then each solution with the same path γ, i.e., every solution $x_s(t + \alpha)$ for $\alpha \in \mathbb{R}$, is orbitally stable too.

Definition A.2 (Asymptotic Orbital Stability): The solution $x_s(t)$ of (56) is said to be asymptotically orbitally stable if it is orbitally stable and if a $\delta > 0$ exists such that $\text{dist}(x_0, \gamma) < \delta$ implies

$$\text{dist}(\phi(t, x_0), \gamma) \to 0 \text{ as } t \to \infty.$$

Definition A.3 (Asymptotic Phase Property): The solution $x_s(t)$ is said to have the asymptotic phase property if a $\delta > 0$ exists such that to each initial value x_0 satisfying $\text{dist}(x_0, \gamma) < \delta$ there corresponds an asymptotic phase $\alpha(x_0) \in \mathbb{R}$ with the property

$$\lim_{t \to \infty} |\phi(t, x_0) - x_s(t + \alpha(x_0))| = 0.$$

For the autonomous systems we are dealing in this work, we assume that there exists a nontrivial periodic solution $x_s(t)$ which is asymptotically orbitally stable and has the asymptotic phase property.

Appendix B
Floquet Theory

Consider the n-dimensional inhomogeneous linear system of differential equations

$$\dot{x} = A(t)x + b(t) \tag{57}$$

where the matrix function A: $\mathbb{R} \to \mathbb{R}^{n^2}$ and the vector b: $\mathbb{R} \to \mathbb{R}^n$ are continuous. The homogeneous system corresponding to (57) is given by

$$\dot{x} = A(t)x. \tag{58}$$

Remark B.1:

- The conditions of the Picard–Lindelőf existence and uniqueness theorem [23] for initial value problems are trivially satisfied by (57) and (58). Hence, there exist unique solutions to (57) and (58) given an initial condition $x(t_0) = x_0$.
- It can be shown that the set of real solutions of (58) form an n-dimensional linear space.
- Let $x_1(t, t_0), \cdots, x_n(t, t_0)$ be n linearly independent solutions of (58). Then, $X(t, t_0) = [x_1(t, t_0), \cdots, x_n(t, t_0)]$ is called a fundamental matrix. If $X(t_0, t_0) = I_n$, then $X(t, t_0)$ is called the principal fundamental matrix or the state transition matrix for (58), denoted by $\Phi(t, t_0)$.
- Any solution of (58) can be expressed as $X(t, t_0)c$ where $c \neq 0$ is a constant vector. In particular, for $x(t_0) = x_0$, the solution of (58) is given by $\Phi(t, t_0)x_0$.
- If $\tilde{X}(t, t_0)$ is another fundamental matrix for (58), then $\tilde{X}(t, t_0) = X(t, t_0)C$ where C is a nonsingular constant matrix.
- The solution ϕ of (57) satisfying the initial condition $x(t_0) = x_0$ is given by

$$\phi(t, t_0, x_0) = \Phi(t, t_0)x_0 + \int_{t_0}^{t} \Phi(t, s)b(s)\, ds. \tag{59}$$

Now we consider the case when the coefficient matrix in (58) is periodic with period $T > 0$, i.e., $A(t + T) = A(t)$ for $t \in \mathbb{R}$. Let $X(t, t_0)$ be a fundamental matrix for (58).

Remark B.2:

- Consider $X(t + T, t_0)$. We have

$$\dot{X}(t + T, t_0) = A(t + T)X(t + T, t_0) = A(t)X(t + T, t_0)$$

hence, $X(t+T, t_0)$ is also a fundamental matrix. Then, $X(t+T, t_0) = X(t, t_0)B$ where B is a nonsingular matrix. Note that $B = X^{-1}(t_0, t_0)X(t_0+T, t_0)$.

- Even though B is not unique, it can be shown that any other B will have the same eigenvalues.
- The eigenvalues of B, $\lambda_1, \cdots, \lambda_n$, are called the characteristic multipliers of the equation and the characteristic (Floquet) exponents $\mu_1, \cdots, \mu_n$ are defined with $\lambda_i = \exp(\mu_i T)$.

Assumption B.1: We assume that B has distinct eigenvalues and it is diagonalizable.[12]

Now we state a result due to Floquet (1883).

Theorem B.1 (Floquet): Let $B = W\Lambda W^{-1}$ where $\Lambda = \exp(DT)$, $D = \text{diag}[\mu_1, \cdots, \mu_n]$, and $\Lambda = \text{diag}[\lambda_1, \cdots, \lambda_n]$. Then, the state transition matrix of the system (58) can be written in the form

$$\Phi(t, s) = U(t)\exp(D(t-s))V(s)$$

where $U(t)$ and $V(t)$ are both T-periodic and nonsingular and satisfy

$$U(t) = V^{-1}(t).$$

Proof: [23]. ∎

Remark B.3:

- The state transition matrix $\Phi(t, s)$ can be written as

$$\Phi(t, s) = \sum_{i=1}^{n} \exp(\mu_i(t-s))u_i(t)v_i^T(s)$$

where $u_i(t)$ are the columns of $U(t)$ and $v_i^T(t)$ are the rows of $V(t) = U^{-1}(t)$.

- With this representation of the state transition matrix, the solutions of the homogeneous system (58) and the inhomogeneous system (57) with a periodic coefficient matrix are given by

$$x_H(t) = \sum_{i=1}^{n} \exp(\mu_i(t-t_0))u_i(t)v_i^T(t_0)x(t_0)$$

and

$$x_{IH}(t) = x_H(t) + \sum_{i=1}^{n} u_i(t) \int_{t_0}^{t} \cdot \exp(\mu_i(t-s))v_i^T(s)b(s)\,ds.$$

- For any i, $x(t) = u_i(t)\exp(\mu_i t)$ is a solution of (58) with the initial condition $x(t_0) = u_i(t_0)\exp(\mu_i t_0)$. Similarly, $x(t) = v_i(t)\exp(-\mu_i t)$ is a solution of the adjoint system

$$\dot{x} = -A^T(t)x$$

with the initial condition $x(t_0) = v_i(t_0)\exp(-\mu_i t_0)$.

- We have

$$\Phi(T, 0) = \sum_{i=1}^{n} \exp(\mu_i T)u_i(T)v_i^T(0) = \sum_{i=1}^{n} \exp(\mu_i T)u_i(0)v_i^T(0).$$

From the above, $u_i(0)$ are the eigenvectors of $\Phi(T, 0)$ with corresponding eigenvalues $\exp(\mu_i T)$ and $v_i(0)$ are the eigenvectors of $\Phi(T, 0)^T$ corresponding to the same eigenvalues.

APPENDIX C
KRAMERS–MOYAL EXPANSION AND THE FOKKER–PLANCK EQUATION

Let $X(t)$ be a stochastic process with the probability density function (PDF) $f_X(x, t)$.

Definition C.1:

$$D^{(i)}(x, t) = \frac{1}{i!} \lim_{s \to 0} \frac{\mathrm{E}\left[(X(t+s) - X(t))^i \,|\, X(t) = x\right]}{s} \tag{60}$$

where $\mathrm{E}[.|.]$ denotes the conditional expectation operator.

Theorem C.1 (Kramers–Moyal Expansion): The PDF of the stochastic process $X(t)$ satisfies the following partial differential equation:

$$\frac{\partial f X(x, t)}{\partial t} = \sum_{i=1}^{\infty} \frac{\partial^i}{\partial x^i} (-1)^i D^{(i)}(x, t) f_X(x, t) \tag{61}$$

where $D^{(i)}(x, t)$ are given by (60).

Proof: [29], [28]. ∎

(61) is called the Kramers–Moyal expansion and $D^{(i)}(x, t)$ in (60) are called the Kramers–Moyal expansion coefficients.

Now, let the stochastic process $X(t)$ satisfy the following nonlinear stochastic differential equation

$$\dot{X} = h(X, t) + g^T(X, t)b(t) \tag{62}$$

where $b(t)$: $\mathbb{R} \to \mathbb{R}^p$ is a vector of uncorrelated zero mean Gaussian white noise processes $h(x, t)$: $\mathbb{R} \times \mathbb{R} \to \mathbb{R}$ and $g(x, t)$: $\mathbb{R} \times \mathbb{R} \to \mathbb{R}^p$ are deterministic functions.

Theorem C.2: For the stochastic process $X(t)$ that satisfies (62), the Kramers–Moyal expansion coefficients defined by (60) are given by

$$\begin{aligned} D^{(1)}(x, t) &= h(x, t) + \lambda \frac{\partial g^T(x, t)}{\partial x} g(x, t) \\ D^{(2)}(x, t) &= \tfrac{1}{2}\, g^T(x, t)g(x, t) \\ D^{(i)} &= 0 \text{ for } i > 2 \end{aligned}$$

where $0 \le \lambda \le 1$ depends on the definition of the stochastic integral [25], [26], [28] used to interpret the stochastic differential equation in (62).

Proof [29], [28], [25]: Hence, the partial differential equation, i.e., the Kramers–Moyal expansion, for the PDF of $X(t)$ that satisfies (62) can be written as

$$\begin{aligned} &\frac{\partial f_X(x, t)}{\partial t} \\ &= -\frac{\partial}{\partial x}\left(h(x, t)f_X(x, t) + \lambda \frac{\partial g^T(x, t)}{\partial x} g(x, t) f_X(x, t)\right) \\ &\quad + \frac{1}{2}\frac{\partial^2}{\partial x^2}(g^T(x, t)g(x, t)f_X(x, t)) \end{aligned} \tag{63}$$

which is known as the Fokker–Planck equation or the forward Kolmogorov equation.

[12]The extension to nondiagonalizable matrices is straightforward.

The phase deviation α satisfies the stochastic differential (12). We obtain the Fokker–Planck equation (21) for the PDF $p_\alpha(\eta, t)$ of α by substituting $h(x, t) = 0$ and

$$g^T(x, t) = v^T(t+\eta) = v_1^T(t+\eta)B(x_s(t+\eta))$$

in (63).

ACKNOWLEDGMENT

The authors would like to thank L. Toth, P. Vancorenland, P. Kinget, P. Feldmann, B. Melville, D. Long, M. Banu, and A. Hajimiri for technical discussions. They would also like to thank F. Bruckstein for philosophical guidance. They would especially like to acknowledge the pioneering works of F. Kärtner and M. Lax which had a strong influence on this work.

REFERENCES

[1] J. Roychowdhury, "Multi-time analysis of mode-locking and quasiperiodicity in forced oscillators," Bell Laboratories, Murray Hill, NJ, Tech. Memo., 1997.
[2] D. B. Leeson, "A simple model of feedback oscillator noise spectrum," *Proc. IEEE*, vol. 54, no. 2, p. 329, Feb. 1966.
[3] W. P. Robins, *Phase Noise in Signal Sources*. London, U. K.: Peter, 1991.
[4] U. L. Rohde, *Digital PLL Frequency Synthesizers: Theory and Design*. Englewood Cliffs, NJ: Prentice-Hall, 1983.
[5] J. R. Vig, "Quartz crystal resonators and oscillators for frequency control and timing applications," Army Research Lab., 1994.
[6] B. Razavi, "Analysis, modeling and simulation of phase noise in monothilic voltage-controlled oscillators," in *Proc. IEEE Custom Integrated Circuits Conf.*, May 1995.
[7] E. Hafner, "The effects of noise in oscillators," *Proc. IEEE*, vol. 54, no. 2, p. 179, February 1966.
[8] K. Kurokawa, "Noise in synchronized oscillators," *IEEE Trans. Microwave Theory Tech.*, vol. MTT-16, pp. 234–240, Apr., 1968.
[9] V. Rizzoli, A. Costanzo, F. Mastri, and C. Cecchetti, "Harmonic-balance optimization of microwave oscillators for electrical performance, steady-state stability, and near-carrier phase noise," in *IEEE MTT-S Int. Microwave Symposium Dig.*, May 1994.
[10] M. Okumura and H. Tanimoto, "A time-domain method for numerical noise analysis of oscillators," in *Proc. ASP-DAC*, Jan. 1997.
[11] T. C. Weigandt, B. Kim, and P. R. Gray, "Analysis of timing jitter in cmos ring-oscillators," in *Proc. IEEE ISCAS*, June 1994.
[12] J. A. McNeill, "Jitter in ring oscillators," Ph.D. dissertation, Boston Univ., 1994.
[13] A. A. Abidi and R. G. Meyer, "Noise in relaxation oscillators," *IEEE J. Solid-State Circuits*, Dec. 1983.
[14] M. Lax, "Classical noise. V. Noise in self-sustained oscillators," *Phys. Rev.*, vol. CAS-160, pp. 290–307, 1967.
[15] G. Foschini, "Characterizing filtered light waves corrupted by phase noise," *IEEE Trans. Inform. Theory*, vol. 34, Nov. 1988.
[16] V. C. Vannicola and P. K. Varshney, "Spectral dispersion of modulated signals due to oscillator phase instability: White and random walk phase model," *IEEE Trans. Commun.*, vol. COM-31, July 1983.
[17] F. K. Kärtner, "Analysis of white and $f^{-\alpha}$ noise in oscillators," *Int. J. Circuit Theory Appl.*, vol. 18, pp. 485–519, 1990.
[18] A. Hajimiri and T. H. Lee, "A state–space approach to phase noise in oscillators," Lucent Technologies, Tech. Memo., July 1997.
[19] ——, "A general theory of phase noise in electrical oscillators," *IEEE J. Solid-State Circuits*, vol. 33, pp. 179–194, Feb. 1998.
[20] A. Demir and J. Roychowdhury, "On the validity of orthogonally decomposed perturbations in phase noise analysis," Bell Labs., Murray Hill, NJ, Tech. Memo., 1997.
[21] A. Demir, "Phase noise in oscillators: DAE's and colored noise sources," in *Proc. IEEE/ACM Int. Conf. CAD*, Nov. 1998.
[22] ——, "Floquet theory and nonlinear perturbation analysis for oscillators with differential-algebraic equations," Int. J. Circuit Theory Appl., Mar-Apr. 2000, to be published.
[23] M. Farkas, *Periodic Motions*. Berlin, Germany: Springer-Verlag, 1994.
[24] R. Grimshaw, *Nonlinear Ordinary Differential Equations*. New York: Blackwell Scientific, 1990.
[25] L. Arnold, *Stochastic Differential Equations: Theory and Applications*. New York: Wiley, 1974.
[26] *Handbook of Stochastic Methods for Physics, Chemistry and the Natural Sciences*, Springer-Verlag, Berlin, Germany, 1983.
[27] G. R. Grimmet and D. R. Stirzaker, *Probability and Random Processes*, 2nd ed. New York: Oxford Science, 1992.
[28] H. Risken, *The Fokker–Planck Equation*. Berlin, Germany: Springer-Verlag, 1989.
[29] A. Demir, A. Mehrotra, and J. Roychowdhury, "Phase noise in oscillators," Bell Labs., Murray Hill, NJ, Tech. Memo., 1997.
[30] W. A. Gardner, *Introduction to Random Processes with Applications to Signals & Systems*, 2nd ed. New York: McGraw-Hill, 1990.
[31] K. S. Kundert, J. K. White, and A. Sangiovanni-Vincentelli, *Steady-State Methods for Simulating Analog and Microwave Circuits*. Amsterdam, The Netherlands: Kluwer, 1990.
[32] T. J. Aprille and T. N. Trick, "Steady-state analysis of nonlinear circuits with periodic inputs," *Proc. IEEE*, vol. 60, pp. 108–114, Jan. 1972.
[33] ——, "A computer algorithm to determine the steady-state response of nonlinear oscillators," *IEEE Trans. Circuit Theory*, vol. CT-19, pp. 354–360, July 1972.
[34] R. Telichevesky, K. S. Kundert, and J. White, "Efficient steady-state analysis based on matrix-free Krylov-subspace methods," in *Proc. Design Automation Conf.*, June 1995.
[35] J. Roychowdhury, D. Long, and P. Feldmann, "Cyclostationary noise analysis of large RF circuits with multi-tone excitations," *IEEE J. Solid-State Circuits*, Apr. 1998.
[36] A. Dec, L. Toth, and K. Suyama, "Noise analysis of a class of oscillators," *IEEE Trans. Circuits Syst.*, vol. vol. 45, pp. 757–760, June 1998.
[37] P. R. Gray and R. G. Meyer, *Analysis and Design of Analog Integrated Circuits*, 2nd ed. New York: Wiley, 1984.
[38] P. Kinget, "Private Communication," unpublished, June 1997.

Alper Demir was born in Konya, Turkey, in 1969. He received the B.S. degree in electrical engineering from Bilkent University, Turkey, in 1991 and the M.S. and Ph.D. degrees in electrical engineering and computer sciences from the University of California, Berkeley, in 1994 and 1997 respectively.

From May 1992 to January 1997 he worked as a Research and Teaching Assistant in the Electronics Research Laboratory and the EECS department at the University of California, Berkeley. He was with Motorola, Inc. during the summer 1995 and with Cadence Design Systems during the summer 1996. He joined the Research Division of Bell Laboratories, Lucent Technologies as a Member of the Technical Staff in January 1997, where he has been since. His research interests include stochastic modeling and numerical methods for the design and analysis of electronic circuits and systems, and noise analysis for communication circuits.

Dr. Demir received the Regents Fellowship from the University of California at Berkeley, in 1991 and was selected to be an Honorary Fellow of the Scientific and Technical Research Council of Turkey .

Amit Mehrotra received the B. Tech. degree in electrical engineering from the Indian Institute of Technology, Kanpur, India, in 1994 and the M.S. and Ph.D. degrees from the University of California at Berkeley in 1996 and 1999, respectively.

He has joined the Electrical and Computer Engineering department at the University of Illinois at Urbana-Champaign as an Assistant Professor and Research Assistant Professor with the Coordinated Science Laboratory. His research interests include design and simulation of RF, analog and mixed signal circuits and systems, interconnect performance and modelling issues in VLSI and novel circuits and physical design techniques for high-performance DSM VLSI designs.

Jaijeet Roychowdhury received B.Tech. degree from the Indian Institute of Technology, Kanpur, India, in 1987, and the PhD degree from the University of California at Berkeley in 1992.

From 1992 to 1995, he was with the CAD Laboratory of AT&T Bell Laboratories in Allentown, PA. Since 1995, he has been with the Communication Sciences Research Division of Lucent Technologies' Bell Laboratories in Murray Hill, NJ. His interests are in multitime simulation, reduced-order modelling, and noise issues in communications design.